Journal of Geosciences, Osaka City University
Vol. 45, Art. 8, p. 101-123, March, 2002

Detailed stratigraphy of the GS-K2 and GS-K3 drilling cores mainly based on the correlation of volcanic ashes in the northwestern part of the Osaka sedimentary basin, Southwestern Japan

KOBAYASHI Gaku*, MITAMURA Muneki*, YOSHIKAWA Shusaku*, KATOH Shigehiro** and HYODO Masayuki***

*Department of Geosciences, Faculty of Science, Osaka City University, Osaka 558-8585, Japan
** Museum of Nature and Human Activities, Hyogo, Sanda 669-1546, Japan
*** Research Center for Inland Seas, Kobe University, Kobe 657-8501, Japan

Abstract

The Osaka sedimentary basin is a Cenozoic tectonic subsidence basin including Osaka Bay and the Osaka Plain, and is filled with thick deposits: the Pliocene to Pleistocene Osaka Group, middle to upper Pleistocene terrace deposits and upper Pleistocene to Holocene alluvial deposits. After the 1995 Hyogoken-Nanbu Earthquake, many organizations surveyed the subsurface geology and underground structure in the Kobe area. The GS-K2 and GS-K3 cores were drilled at the southern foot of the Rokko Mountains, at Ishiyagawa, Nada-ku, Kobe City. But, because these cores consist of thick gravel beds on the upper parts, many stratigraphic problems have been unsolved. The purpose of this paper is to provide a better stratigraphy of these cores, especially of the upper parts, by means of magnetostratigraphy and correlation of the volcanic ashes with the known marker tephra layers in the Osaka sedimentary basin.

In the GS-K2 core, 2 volcanic ash horizons were identified at depths of 349 m and 11 m, as well as a volcanic ash layer at depth of 181 m. The K2-349 volcanic ash horizon is correlated with Sayama volcanic ash layer for the similarities of shapes of glass shards and its refractive index. As a result of this correlation, the marine sand bed, at depth from 330.0 to 323.2 m is correspondent to the Ma 4 bed. The measurement of the paleomagnetism of the GS-K2 core confirms the marine sand bed correlative with the Ma 4 bed. In the GS-K3 core, 16 volcanic ash layers were found and 6 volcanic ash horizons, 2 approximate volcanic ash horizons and 2 crystal ash horizons were determined. Four volcanic ash layers and 3 volcanic ash horizons in the K3-M unit, and one volcanic ash layer and 2 volcanic ash horizons in the K3-U unit are newly correlated with known volcanic ash layers. The volcanic ashes of the K3-558.9/K3-558.1, K3-520, K3-359, K3-355.4, K3-355.1, K3-291, K3-242, K3-195, K3-180 and K3-15 are equivalent to the K1-648/Yellow Ⅱ/Ⅲ, K1-610/YU277/OT161, Toyodaike, K1-422/Sayama, K1-421, K1-348/Hacchoike Ⅱ, Sakura, K1-245/Kasuri, K1-223/Minatojima Ⅰ and K1-26/Heian-jingu volcanic ash layers, respectively. On the basis of these tephra correlations, 12 marine beds of the K3-M and K3-U are equivalents of the Ma -1, Ma 0, Ma 0.5, Ma 1, Ma 1.3, Ma 1.5, Ma 2, Ma 3, Ma 4, Ma 5, Ma 6, Ma 7 and Ma 9, in ascending stratigraphic order.

Key-words : Osaka sedimentary basin, Quaternary, stratigraphy, Kobe, drilling core, volcanic ash

1. Introduction

The Osaka sedimentary basin in southwestern Japan is a Cenozoic tectonic subsidence basin which includes Osaka Bay and the Osaka Plain. The basin is filled with thick deposits: the Pliocene to Pleistocene Osaka Group, middle to upper Pleistocene terrace deposits and upper Pleistocene to Holocene alluvial deposits, which overlie the pre-Paleogene basement rocks (Itihara, 1993). Excellent stratigraphy of the sediments was established mainly in hilly areas of the basin using volcanic ash layers and marine clay beds as good key layers (Itihara, 1960, 1993 ; Itihara et al., 1988). However, because the sediments are thinner and more discontinuous in the hilly areas than in central part of the basin, a good understanding of the subsurface geology in the central part have been necessary to elucidate the whole stratigraphy of the Osaka sedimentary basin.

After the 1995 Hyogoken-Nanbu Earthquake, many organizations surveyed the subsurface geology and underground structure in and around Osaka Bay and collected many deep cores in the Osaka Plain (Yoshikawa et al., 1997, 1998) and the Kobe area (Takemura et al., 1997 ; Geo-Database Information Committee of Kansai, 1998 ; Mitamura et al., 2000). Among these deep cores, the Higashinada 1700-m core (GS-K1 core in abbreviation) is one of the deepest cores that reached the basement rocks within the Osaka sedimentary basin. Biswas et al. (1999) and Yoshikawa et al. (2000) reported the detailed magnetostratigraphy and tephrostratigraphy of this core, respectively.

The GS-K2 and GS-K3 cores were drilled in the southern foot of the Rokko Mountains, at Ishiyagawa, Nada-ku, Kobe City, northwest of the GS-K1 core site (Fig. 1). Both deep drilling cores are very important for considering the island subsurface stratigraphy. Geo-Database Information Committee of Kansai (1998) and Kobayashi et al. (2001) reported the stratigraphic outline of the two cores, but many points remain unclear particularly in the upper parts of these cores that dominate thick gravel layers and coarsen upward.

The purpose of this paper is first to describe the volcanic ashes of both cores and the paleomagnetism of

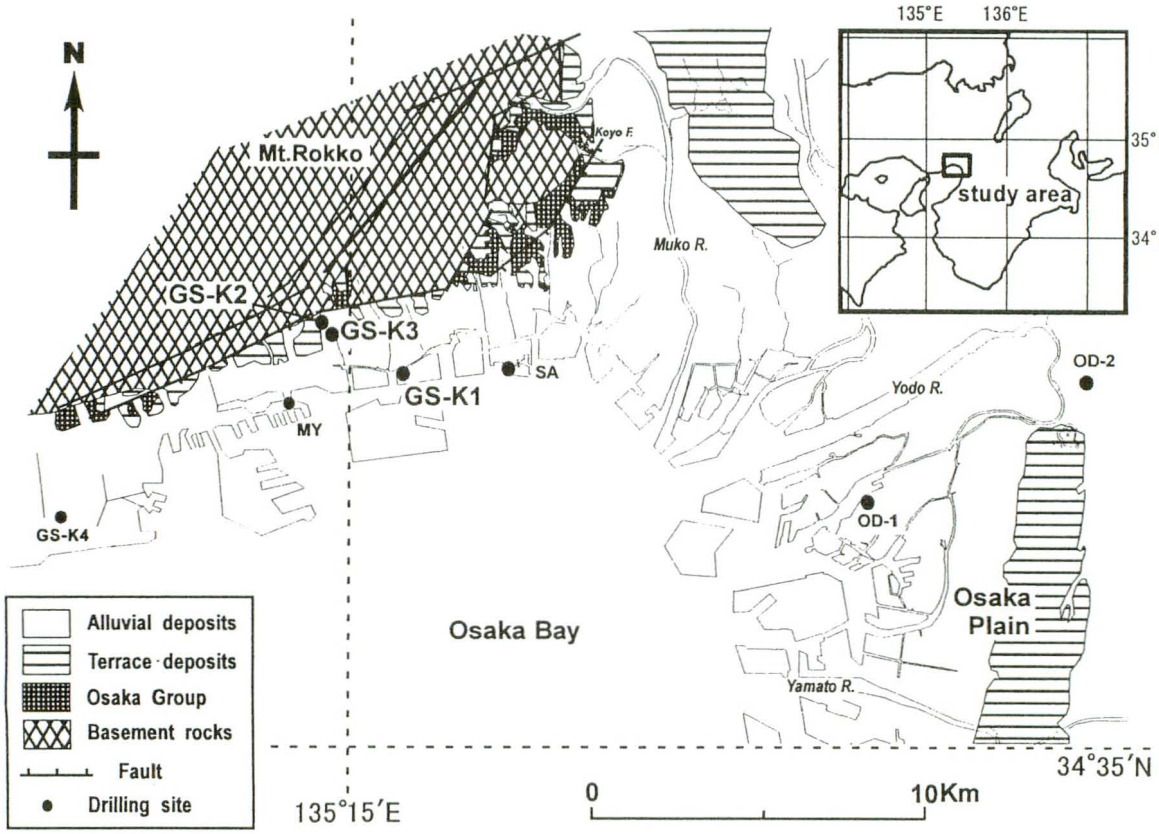

Fig. 1 Geological outline map in the northern part of the Osaka sedimentary basin (modified after Itihara, 1993) and localities of the drilling sites. SA, GS-K1, GS-K2, GS-K3, MY and GS-K4 (Geo-Database Information Committee of Kansai, 1998) indicate the deep drilling sites in the Kobe area. OD-1 and OD-2 (Mitamura et al., 1998) indicate the major deep drilling sites in the Osaka Plain.

the GS-K2 core, and then to provide a better stratigraphy of these cores, especially of the upper parts, by means of magnetostratigraphy and correlation of the volcanic ashes with the known marker tephra layers in the Osaka sedimentary basin.

2. Quaternary stratigraphy of the Osaka sedimentary basin

A standard subsurface stratigraphy under the Osaka sedimentary basin has been proposed by analyzing nine deep drilling cores (OD-1～OD-9) in the Osaka Plain (Ikebe et al., 1970 ; Yoshikawa et al., 1987 ; Mitamura et al., 1998). It shows that the Quaternary sediments under the basin are more than 1,000 m in thickness and consist of unconsolidated clay, silt, sand and gravel, with 17 marine clay beds and scores of volcanic ash layers (Ikebe et al., 1970 ; Kajiyama and Itihara, 1972 ; Yoshikawa et al., 1987 ; Furutani, 1989). Geological studies in the hilly areas of the basin have also led to the stratigraphic division of these sediments into the Osaka Group, the Terrace Formation and the Alluvium Formation (Itihara, 1993). Correlation of this division with the subsurface stratigraphy has been attempted using the marker volcanic ash layers and marine clay beds.

Recently, Yoshikawa et al. (1997, 1998) re-examined the lithology of nine deep drilling cores and newly recognized 4 marine clay beds named the Ma 0.5, Ma 1.3, Ma 1.5, and Ma 1.7 in ascending order. Thus, 21 marine clay beds totally has been recognized in the Osaka sedimentary basin. Yoshikawa and Mitamura (1999) divided the late Cenozoic sediments in the Osaka Plain into three units : the late Pliocene to early Pleistocene Miyakojima Formation, the early Pleistocene to late Pleistocene Tanaka Formation, and the late Pleistocene to Holocene alluvial deposits. Further, the 21 marine clay beds , each of which represents a marine transgression in the Tanaka Formation and alluvial deposits, were considered to be deposited during interglacial high sea-level periods after the Oxygen Isotope Stage 37 (Yoshikawa and Mitamura, 1999).

On the other hand in the Kobe area, there was no deep drilling core for geological investigation before the 1995 Hyogoken-Nanbu Earthquake. Large-scale geological surveys after this earthquake revealed the similar lithofacies of the subsurface sediments in this area with those in the Osaka Plain (Geo-Database Information Committee of Kansai, 1998).

3. Lithofacies of the GS-K2 and GS-K3 cores

The GS-K2 and GS-K3 cores consist of unconsolidated clay, silt, sand and gravel of freshwater, brackish or marine origin. According to Geo-Database Information Committee of Kansai (1998) and Kobayashi et al (2001), the outline of the lithofacies is summarized below. The detailed lithofacies are shown in Fig. 2 and Fig. 3.

3-1. GS-K2 core

The GS-K2 core consists of two lithostratigraphic units of the K2-L (354 to 239.5 m at depths) and K2-U (239.5 to 0.6 m at depths) (Fig. 2). The K2-L unit mainly comprises alternating beds of terrestrial silt, sand, and gravel, with 3 marine beds at depths of 330.0 to 323.2 m, 286.0 to 280.6 m, and 246.2 to 239.5 m. The marine beds are very fine to fine sand in size or consist of medium to coarse sand with silt. Silt beds are 0.1 to 2 m thick and contain fine to medium sand and granule grains. Sand beds mainly consist of medium to coarse sand with granule grains, intercalating peat seams. Gravel beds 1 to 6 m thick, consist mainly of granitic, rhyolitic, andesitic, and chert clasts that range in diameter from 4 to 10 mm (150 mm at max.), and medium to coarse granitic sand as matrix.

The K2-U unit dominates thick gravel beds partially alternating with silt and sand, and includes a single volcanic ash layer. Gravel beds are 1 to 8 m thick and consist mainly of granitic, rhyolitic, and andesitic clasts with diameters of 4 to 40 mm (300 mm at max.) and include medium to coarse granitic sand as matrix, with partially interleaving silt seams. Sand beds are 0.1 to 1 m thick and are composed of very fine to fine sand with silt or medium to coarse sand with granule grains. Silt beds less than 1 m thick are occasionally interleaved in the sand and gravel beds.

3-2. GS-K3 core

The GS-K3 core consists of three lithostratigraphic units of the K3-L, K3-M and K3-U at depths of 680 to 598.4 m, 598.4 to 227.7 m, and 227.7 to 3.1 m, respectively (Fig. 3). The K3-L unit is composed mainly of silt, sand, and gravel beds of freshwater origin and interleaves 2 volcanic ash layers. Silt beds are 0.1 to 2 m thick and contain fine to medium sand and partially carbonaceous silt. Sand beds 1 to 4 m thick consist of fine to very coarse with silt seams. Gravel beds 2 to 5 m thick consist of medium to coarse sand and granitic chert clasts with diameters of 2 to 30 mm.

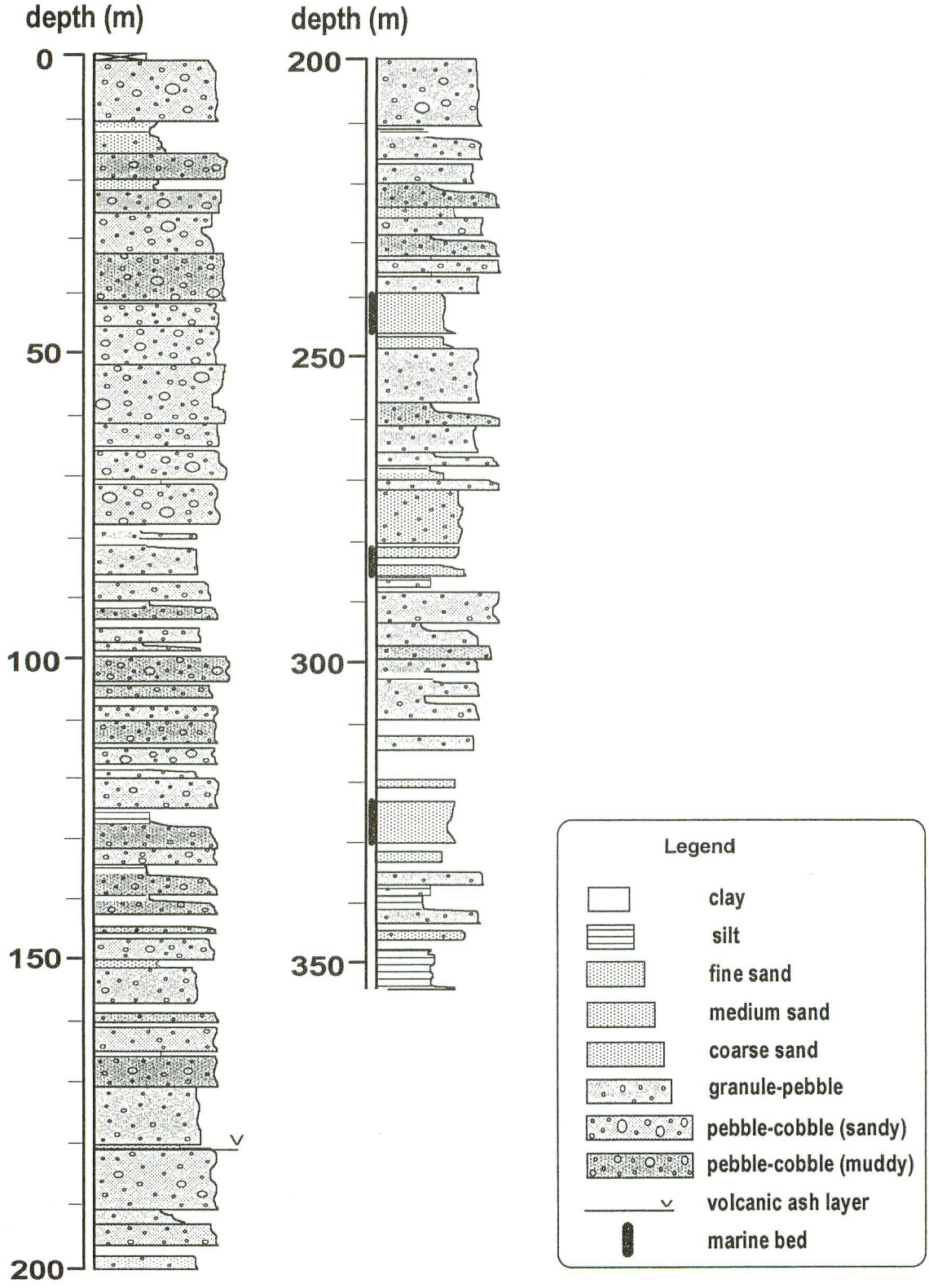

Fig. 2 Columnar section of the GS-K2 drilling core.

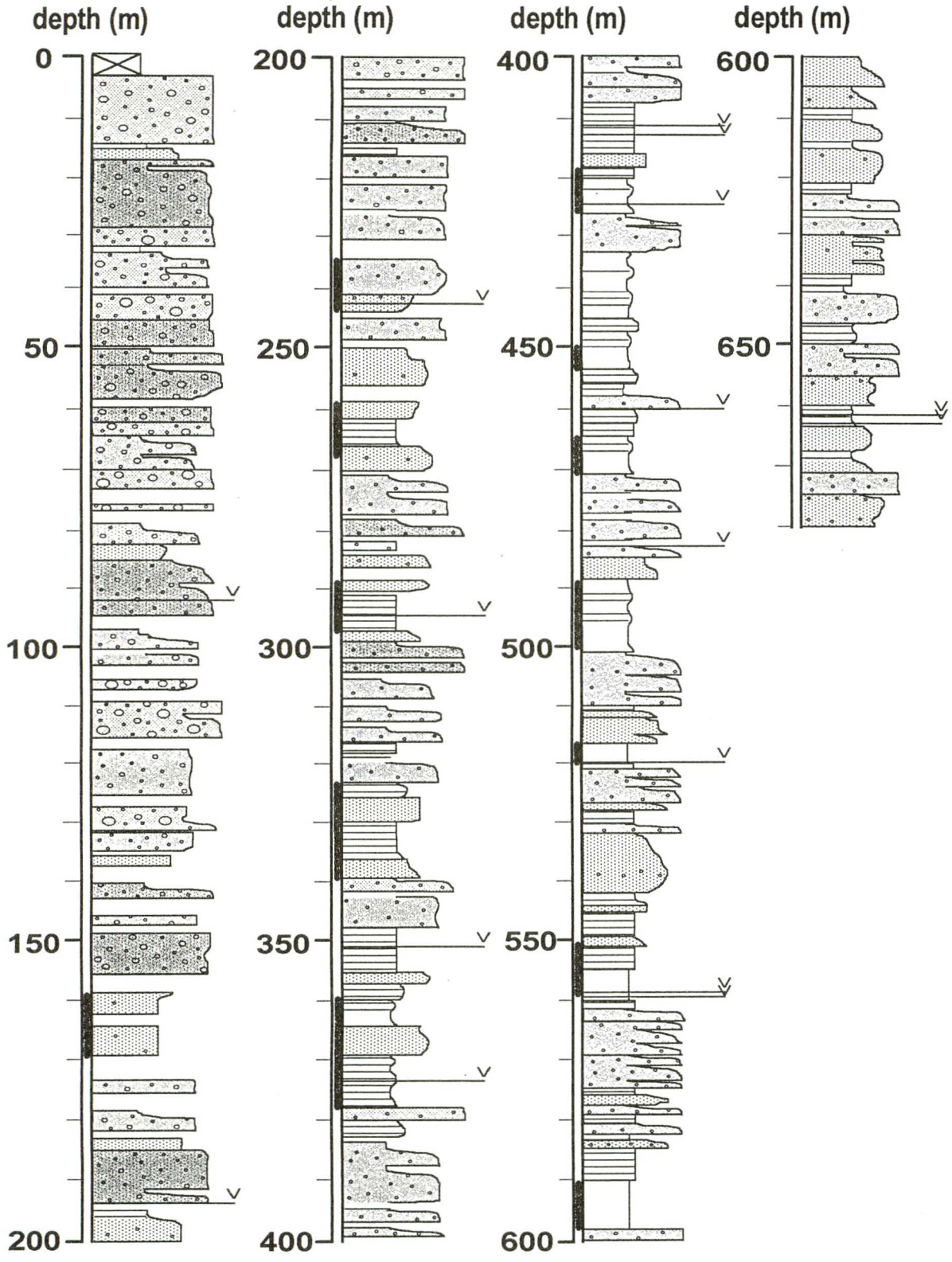

Fig. 3 Columnar section of the GS-K3 drilling core.

The K3-M unit comprises alternating beds of terrestrial silt, sand, and gravel with 12 marine beds and 12 volcanic ash layers (Fig. 3). The marine beds range in thickness from 5 to 10 m and mainly consist of clay and silt, partially interleaving seams of fine sand. Sand beds are medium to coarse in size and partially contain gravel. Gravel beds are 1 to 8 m thick and consist mainly of medium to coarse sand and granitic, rhyolitic, and chert clasts with diameters from 2 to 10 mm (40 mm at max.).

The K3-U unit is dominated by thick gravel beds partially alternating with silt and sand, and an interleaved single marine bed and 2 volcanic ash layers. The marine bed at a depth of 168.9 to 158.9 m, consists of fine sand with granule grains. Silt beds less than 1 m thick contain carbonaceous silt and fine sand. Sand beds are less than 1 m thick and are medium to coarse in size. Gravel beds are 1 to 5 m thick and consist mainly of granitic, rhyolitic, andesitic, and chert clasts with medium to coarse granitic sand matrix. Diameters of the clasts vary from 4 to 20 mm, and reach 150 mm at maximum.

4. Petrographic properties of the volcanic ash layers and volcanic ash horizons

4-1. Analytical methods

The single volcanic ash layer in the GS-K2 core and 16 volcanic ash layers in the GS-K3 core were described concerning thickness, color, grain size, lithofacies and so on. Then, samples of 5 to 20 g taken from the 17 volcanic ash layers, and from clay, silt, and fine- or medium-sand parts of the two cores at 0.3 to 2 m intervals were analyzed following Yoshikawa (1984).

The samples were dried below 50 ℃ and weighed. After disaggregation and cleaning in water using an ultrasonic cleaner, they were wet-sieved using 63 meshes (1/4 mm) and 250 meshes (1/16 mm) Tyler screen, and dried and weighed. The fine-sand size fractions between 1/4 and 1/16 mm were mounted on glass slides and more than 200 grains were counted under a polarizing microscope to determine the percentage of volcanic glass shards, plagioclase, quartz, heavy mineral and other grains (volcanic fragments, accidental fragments and so on). Heavy minerals between 1/4 and 1/16 mm were further separated by ethanol solution of bromoform with a specific gravity of 2.85. The heavy minerals were mounted on glass slides and more than 200 grains were counted under a microscope to determine the percentage of grains of amphibole, orthopyroxene, clinopyroxene, biotite, zircon, apatite and opaque minerals.

Yoshikawa (1976) classified a wide variety of glass shard shapes into three representative types. The first type (H-type shard) consists of plate shards as broken walls of relatively large bubbles. The second type (T-type shard) contain numerous small bubbles or are fibrous, and represent pumice fragments. The third type (C-type shard) is an intermediate form between the H-type and the T-type shards. The types of at least 200 glass shards were classified into the three types and others and the percentage of the four classifications were determined. Refractive index of the glass shards and heavy mineral crystals were measured by the dispersion-coloration technique, using a set of standard glass shards and an optical phase-microscope. The accuracy of this technique is estimated less than ± 0.001 (Yoshikawa, 1976).

4-2. Determination of volcanic ash horizon in the core sediments

Yoshikawa (1981), Yoshikawa et al. (1993) and Miyakawa et al. (1996) investigated in detail the vertical variation of the contents, shapes and the refractive index of volcanic glass shards of core sediments, and indicated that these parameters were applicable to determination of volcanic ash horizon where a volcanic ash was originally deposited. They decided the volcanic ash horizon with a considerable content of glass shards having characteristic glass type composition and refractive index.

In contrast, Ishihara et al. (1997) used the GS-K4 core that consists mainly of coarse sediments, and determined a horizon at which the content of new glass shards indicates a clear peak within a wide range of minor occurrences. They considered that the glass shards contents were lowered within coarser sediments due to larger transportation power, but the fall of a volcanic ash was recorded by appearance of new types of glass shards if it was few.

The vertical changes in content of fine sand-size fractions in the GS-K2 and GS-K3 core sediments are shown in Figs. 4 and 5. Those of volcanic glass fractions and heavy mineral fractions, limited to grains with euhedral and fresh shards, are also shown in these figures. Because the GS-K2 and GS-K3 cores mainly consist of coarse materials and volcanic glass shards diffuse upward and downward, glass shards appear with lower contents within long ranges of the cores. Consequently in this study, a horizon where volcanic glass shards constitute more than 5 per cent with a clear peak is identified as a volcanic ash horizon.

In the GS-K3 core, two wide ranges are recognized, where glass shards appear at low frequency with no clear peaks of the content. Because large lithological changes are found beneath the ranges, the appearance of new types of glass shards with frequency probably result from wide diffusion of glass shards just after falls of volcanic ashes. Thus, the lowest horizons of the ranges are considered to be approximate volcanic ash horizons.

Furthermore, it exists two horizons in the GS-K3 core that contains no volcanic glass shards but indicate peaks of heavy mineral contents. Dominant minerals, amphibole in both horizons, are euhedral and fresh in sharp and show characteristic refractive index. In this study, those two horizons that heavy minerals constitute more than 5 per cent were considered to indicate falls of volcanic ashes mainly composed of heavy mineral crystals (crystal ash horizons) like those determined based on the vertical variations of glass shards content and morphology and refractive index.

4-3. Description of volcanic ash layers and volcanic ash horizons in the GS-K2 and GS-K3 cores

In the GS-K2 core, two volcanic ash horizons were identified at depths of 349 m and 11 m (K2-349 and K2-11 volcanic ash horizons), as well as a volcanic ash layer (K2-181) at a depth of 181 m (Fig. 4). In the GS-K3 core, 16 volcanic ash layers were found and 6 volcanic ash horizons, 2 approximate volcanic ash horizons and 2 crystal ash horizons were determined as shown in Fig. 5. The petrographic properties of these volcanic ash layers and volcanic ash horizons are also given in Table 1. Distributions of refractive index of volcanic glass are shown in Fig. 6, those of green hornblende are shown in Fig. 7 and those of orthopyroxene are shown in Fig. 8.

4-3-1. GS-K2 core

K2-349 volcanic ash horizon: The K2-349 volcanic ash horizon, in a sandy silt bed, is composed of 9 per cent volcanic glasses and 11 per cent heavy minerals. In the mineral composition, plagioclase, glass, heavy minerals and quartz are common. Glass particles consist mainly of colorless C-type shards with refractive index of 1.506-1.511. In the heavy minerals, amphibole, biotite, opaque minerals, and orthopyroxene are dominant and clinopyroxene is rare.

K2-181 volcanic ash layer: The K2-181 volcanic ash layer, the thickness of which is 3 cm, is composed of gray-colored and medium to coarse grained volcanic ash. In the mineral composition, plagioclase and heavy minerals are abundant. In the heavy minerals, amphibole is dominant, opaque minerals are common and orthopyroxene (γ =1.702-1.714) and apatite are rare. Amphibole particles consist mainly of green and green brown colored shards with refractive index of 1.678-1.690 (n_2) (mode : 1.681).

K2-11 volcanic ash horizon: The K2-11 volcanic ash horizon, in a sand bed, is composed of 24 per cent volcanic glasses and a single per cent heavy minerals. In the mineral composition, plagioclase and glass are abundant and heavy minerals are rare. Glass particles consist mainly of colorless and pale brown H-type and C-type shards with refractive index of 1.509-1.515 (mode : 1.512). In the heavy minerals, orthopyroxene, opaque minerals, and amphibole are dominant, clinopyroxene is common, and biotite and apatite are rare.

4-3-2. GS-K3 core

K3-662 volcanic ash layer: The K3-662 volcanic ash layer, the thickness of which is 2 cm, is composed of white and fine grained volcanic ash. In the mineral composition, glass and plagioclase are abundant, heavy minerals are common and quartz is rare. Glass particles consist mainly of colorless T-type shards with refractive index of 1.503-1.505 (mode : 1.503). In the heavy minerals, amphibole is dominant, opaque minerals are common and apatite, biotite, orthopyroxene and zircon are rare.

K3-661 volcanic ash layer: The K3-661 volcanic ash layer, the thickness of which is 1 cm, is composed of white and fine grained volcanic ash. In the mineral composition, glass and plagioclase are abundant and heavy minerals and quartz are rare. Glass particles consist mainly of colorless T-type shards with refractive index of 1.501-1.504. In the heavy minerals, amphibole is dominant, apatite and opaque minerals are common and orthopyroxene and zircon are rare.

K3-558.9 volcanic ash layer: The K3-558.9 volcanic ash layer, the thickness of which is 2 cm, is composed of white and fine grained volcanic ash. In the mineral composition, glass and plagioclase are abundant, heavy minerals are common and quartz is rare. Glass particles consist mainly of colorless T-type shards with refractive index of 1.500-1.504. In the heavy minerals, amphibole is dominant, apatite, opaque minerals and biotite are common, and orthopyroxene and zircon are rare.

K3-558.1 volcanic ash layer: The K3-558.1 volcanic ash layer, the thickness of which is 2 cm, is composed of gray to white and fine to medium grained volcanic ash. In the mineral composition, glass and

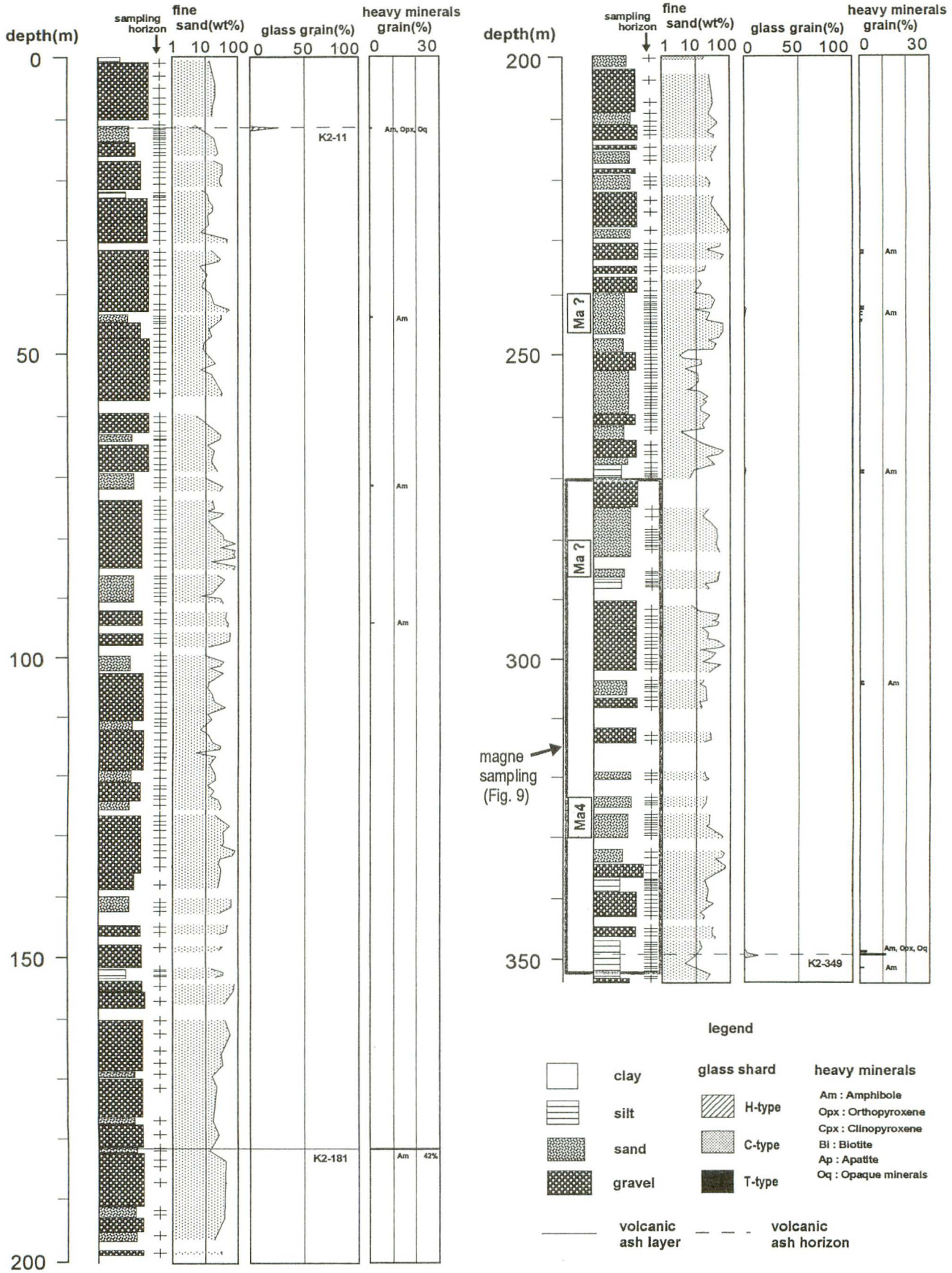

Fig. 4 Vertical variation of the content of fine-sand size fractions, volcanic glass fractions and heavy mineral fractions in the GS-K2 drilling core. Fine-sand size fractions are 1/16 to 1/4 mm in size.

plagioclase are abundant and heavy minerals and quartz are rare. Glass particles consist mainly of colorless T-type shards with refractive index of 1.500-1.504. In the heavy minerals, amphibole is dominant, apatite, opaque minerals and orthopyroxene are common, and biotite is rare.

K3-520 volcanic ash layer: The K3-520 volcanic ash layer, the thickness of which is 2 cm, is composed of gray to yellowish white and fine to medium grained volcanic ash. In the mineral composition, glass, plagioclase and heavy minerals are abundant and quartz is rare. Glass particles consist mainly of colorless T-type shards with refractive index of 1.501-1.503. In the heavy minerals, amphibole is dominant, apatite, opaque minerals and orthopyroxene are common, and biotite is rare.

K3-482 volcanic ash layer: The K3-482 volcanic ash layer, the thickness of which is 5 cm, is composed of yellowish white and fine grained volcanic ash. In the mineral composition, glass is abundant, plagioclase is common and heavy minerals and quartz are rare. Glass particles consist mainly of colorless H- and C-type shards with refractive index of 1.497-1.501 (mode : 1.500-1.501). In the heavy minerals, amphibole is dominant, opaque minerals and orthopyroxene are common and apatite and zircon are rare.

K3-460 volcanic ash layer: The K3-460 volcanic ash layer, about 72 cm thick, consists of five parts; the grey to white, fine grained lowermost part 2 cm thick, the gray to white, medium grained lower part 12 cm thick, the white, fine grained middle part 20 cm thick, the gray to white, fine grained upper part 27 cm thick, and the white, fine grained lowermost part 11 cm thick. In the mineral composition, glass and plagioclase are abundant and heavy minerals and quartz are common. Glass particles consist mainly of colorless and pale brown T-type shards with refractive index of 1.500-1.502 (mode : 1.501). In the heavy minerals, amphibole is dominant, opaque minerals and apatite are common, and biotite is rare.

K3-424 volcanic ash layer: The K3-424 volcanic ash layer, the thick of which is 3 cm, is composed of gray and fine grained volcanic ash. In the mineral composition, glass and plagioclase are abundant and heavy minerals and quartz are rare. Glass particles consist mainly of colorless C- and H-type shards with refractive index of 1.502-1.507. In the heavy minerals, amphibole and opaque minerals are dominant, apatite is common, and biotite and orthopyroxene are rare.

K3-412 volcanic ash layer: The K3-412 volcanic ash layer, about 8 cm thick, consists of three parts; the white, fine grained lower part 2 cm thick, the gray to white, fine grained middle part 1 cm thick, the white, fine grained upper part 5 cm thick. In the mineral composition, glass, plagioclase and heavy minerals are abundant and quartz is rare. Glass particles consist mainly of colorless T-type shards with refractive index of 1.500-1.503 (mode : 1.501). In the heavy minerals, amphibole is dominant and biotite, opaque minerals and apatite are common.

K3-411 volcanic ash layer: The K3-411 volcanic ash layer, about 6 cm thick, consists of two parts; the gray, fine grained lower part 2 cm thick, the white, fine grained upper part 4 cm thick. In the mineral composition, glass is abundant, plagioclase is common and heavy minerals and quartz are rare. Glass particles consist mainly of colorless T-type shards with refractive index of 1.500-1.503. In the heavy minerals, amphibole is dominant, opaque minerals and apatite are common and biotite and orthopyroxene are rare.

K3-373 volcanic ash layer: The K3-373 volcanic ash layer, about 7 cm thick, consists of two parts; the dark gray, fine grained lower part 2 cm thick, the gray, fine to medium grained upper part 5 cm thick. In the mineral composition, glass is abundant, plagioclase is common and heavy minerals are rare. Glass particles consist mainly of colorless and pale brown C-type shards with refractive index of 1.511-1.514. In the heavy minerals, orthopyroxene is dominant and clinopyroxene, amphibole, opaque minerals and apatite are common.

K3-359 volcanic ash horizon: The K3-359 volcanic ash horizon, in a sandy silt bed, is composed of 35 per cent volcanic glasses and 4 per cent heavy minerals. In the mineral composition, glass and plagioclase are abundant and heavy minerals and quartz are rare. Glass particles consist mainly of colorless T-type and C-type shards with refractive index of 1.499-1.504. In the heavy minerals, biotite is dominant, amphibole and opaque minerals are common and orthopyroxene is rare.

K3-355.4 volcanic ash horizon: The K3-355.4 volcanic ash horizon, in a silt bed, is composed of 53 per cent volcanic glasses and 5 per cent heavy minerals. In the mineral composition, glass and plagioclase are abundant and heavy minerals and quartz are common. Glass particles consist mainly of colorless and pale brown H-type and C-type shards with refractive index of 1.508-1.514. In the heavy minerals, orthopyroxene is dominant, amphibole and opaque minerals are common and clinopyroxene and apatite are rare.

K3-355.1 volcanic ash layer: The K3-355.1 volcanic ash layer, about 6 cm thick, consists of two parts;

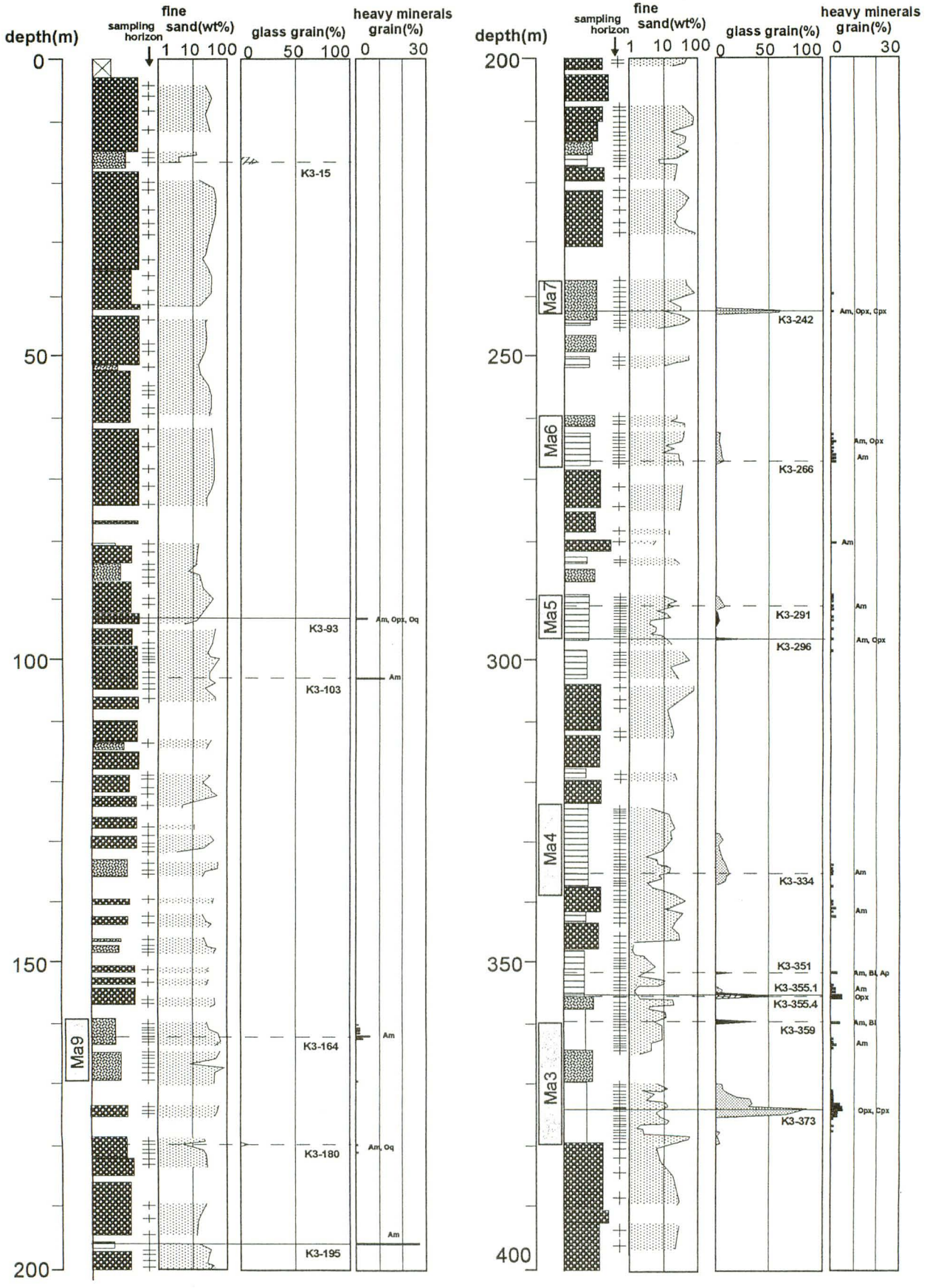

Fig. 5 Vertical variation of the content of fine-sand size fractions, volcanic glass fractions and heavy mineral fractions in the GS-K3 drilling core. Fine-sand size fractions are 1/16 to 1/4 mm in size.

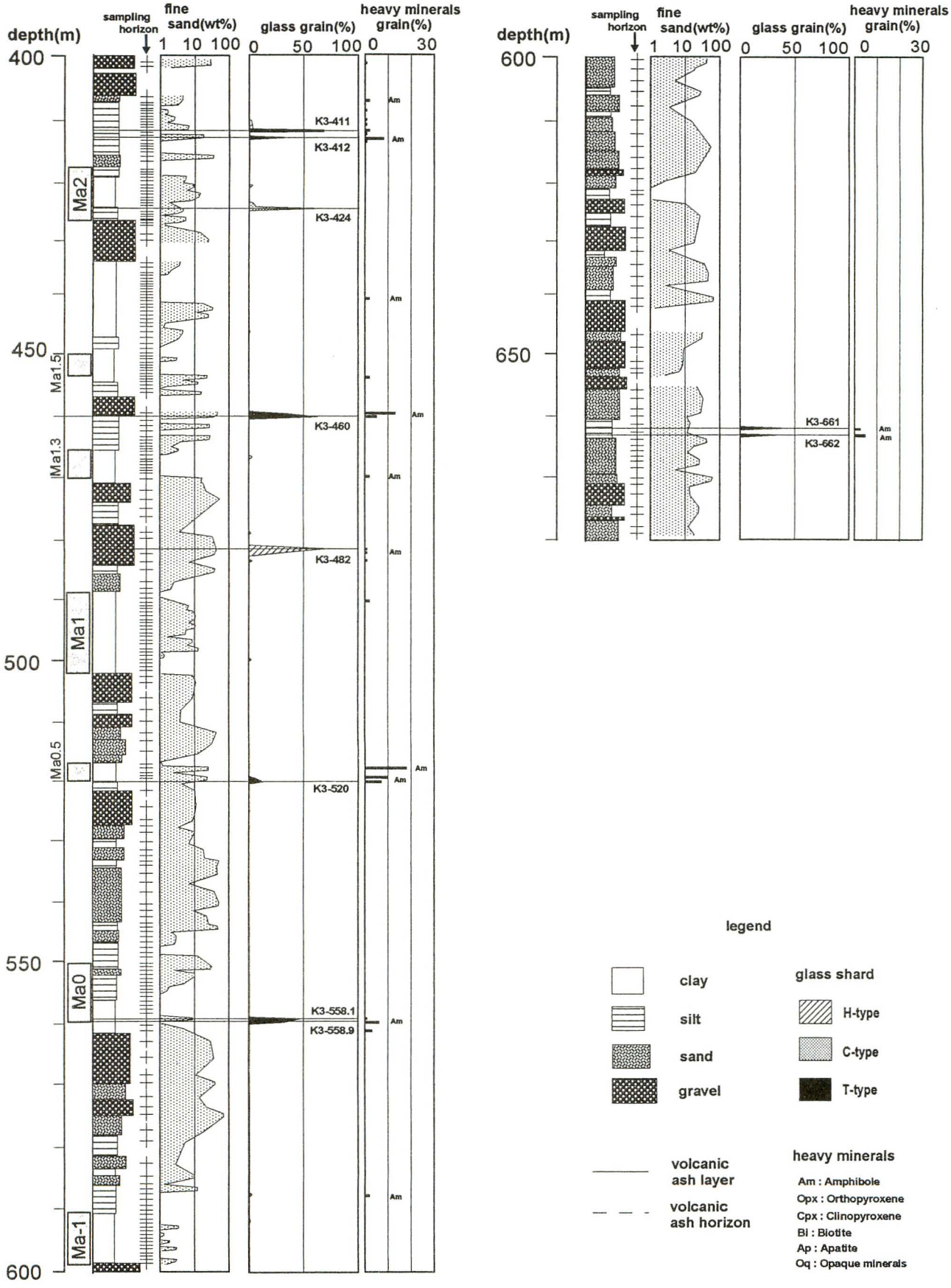
depth(m)
sampling horizon
fine sand(wt%)
1 10 100
glass grain(%)
0 50 100
heavy minerals grain(%)
0 30
400
450
500
550
600
650
Ma2
Ma1.5
Ma1.3
Ma1
Ma0.5
Ma0
Ma-1
K3-411
K3-412
K3-424
K3-460
K3-482
K3-520
K3-558.1
K3-558.9
K3-661
K3-662
Am
legend
clay
silt
sand
gravel
glass shard
H-type
C-type
T-type
volcanic ash layer
volcanic ash horizon
heavy minerals
Am : Amphibole
Opx : Orthopyroxene
Cpx : Clinopyroxene
Bi : Biotite
Ap : Apatite
Oq : Opaque minerals

Table 1 Facies and petrographic properties of volcanic ashes in the GS-K2 and GS-K3 drilling core.

Name of tephra	Facies		Thickness (cm)	Mineral composition					Glass					Heavy mineral composition								Refractive Index	
				Gl	Fl	Qz	Hm	Ot (%)	Sharp				Refractive Index (n) (mode)	Bi	Am	Op	Cp	Zr	Ap	Oq (%)	Am	Op
	color	grain size							H	C	T	O (%)									Index=n_2 (mode)	Index=γ (mode)
K2-11	-	-	-	24	68	*	1	7	70	28	2	0	1.509-1.515 (1.512)	2	21	40	6	0	1	30		
K2-181	gra.	me.sd.-co.sd.	3	0	20	0	42	38						0	82	5	0	0	1	12	1.678-1.690 (1.681)	1.702-1.714
K2-349	-	-	-	9	43	5	11	32	21	53	26	0	1.506-1.511	27	41	16	1	0	0	15		
K3-15	-	-	-	14	71	*	1	14	63	33	4	0	1.498-1.500 (1.500)	*	60	18	1	0	0	21		
K3-93	pur.gra.	v.f.sd.	8	*	14	2	5	78		+				2	32	25	6	1	6	28	1.686-1.691 (1.687)	1.704-1.710 (1.705-1.707)
K3-103	-	-	-	0	53	*	12	35						0	94	*	0	0	1	4	1.674-1.685	
K3-164	-	-	-	0	26	0	6	68						0	91	2	0	0	0	7	1.672-1.682	
K3-180	-	-	-	5	61	1	1	32	50	48	2	0	1.503-1.505	2	60	10	3	0	1	24		
K3-195	gra.	me.sd.-co.sd.	5	0	40	1	27	32						0	86	6	0	0	1	7	1.681-1.691 (1.683)	1.705-1.713
K3-242	whi.gra.	fi.sd.	5	53	41	1	*	5	51	28	21	0	1.502-1.507 (1.506)	4	48	24	16	0	0	8		
K3-266	-	-	-	6	74	*	2	18	18	60	17	5	1.499-1.508	2	69	14	2	2	0	6		
K3-291	-	-	-	8	66	*	1	25	13	60	27	0	1.511-1.517	11	67	4	0	2	3	13		
K3-296	gra.whi.	si.-v.f.sd.	8	24	27	*	*	49	2	9	89	0	1.517-1.521		+	+	+					
K3-334	-	-	-	10	57	5	1	27	3	60	37	0	1.499-1.504	37	42	6	0	0	1	14		
K3-351	-	-	-	13	54	1	3	29	2	42	56	0	1.498-1.511	32	28	4	0	0	20	16		
K3-355.1	gra.whi.	si.-v.f.sd.	6	34	40	2	5	19	5	16	79	0	1.498-1.507	20	65	5	0	0	3	7		
K3-355.4	-	-	-	53	21	4	5	17	36	34	30	0	1.506-1.514	*	12	67	2	0	5	14		
K3-359	-	-	-	35	31	3	4	27	4	35	61	0	1.499-1.504	45	38	*	0	*	0	17		
K3-373	gra.whi.	v.f.sd.-me.sd.	7	65	14	2	5	14	23	45	29	3	1.511-1.514	*	14	50	16	0	10	10		
K3-411	pur.gra.	si.-v.f.sd.	6	68	14	2	2	14	0	11	89	0	1.500-1.503	2	87	1	0	0	4	6		
K3-412	whi.	si.-fi.sd.	8	35	22	3	8	32	0	14	86	0	1.500-1.503 (1.501)	8	81	0	0	0	4	7		
K3-424	pur.gra.	si.-fi.sd.	3	64	23	2	*	11	47	51	0	2	1.502-1.507	1	66	2	0	0	5	26		
K3-460	gra.whi.	si.-me.sd.	72	62	17	3	5	13	0	23	77	0	1.500-1.502 (1.501)	1	88	0	0	0	7	4		
K3-482	yel.whi.	fi.sd.	5	70	17	2	1	10	48	43	9	0	1.497-1.501 (1.500-1.501)	0	83	10	0	1	2	4		
K3-520	yel.gra.	fi.sd.-me.sd.	2	11	67	4	7	11	0	14	85	1	1.501-1.503	1	90	2	0	0	3	4		
K3-558.1	gra.whi.	si.	2	47	41	1	1	10	2	32	64	2	1.500-1.504	1	86	3	0	0	5	5		
K3-558.9	whi.	fi.sd.	2	32	41	2	6	19	3	16	81	0	1.500-1.504	2	87	1	0	1	6	3		
K3-661	whi.	fi.sd.	1	43	20	2	2	33	0	28	72	0	1.501-1.504	0	86	1	0	1	6	6		
K3-662	whi.	fi.sd.	2	38	34	1	4	23	4	12	84	0	1.503-1.505 (1.503)	1	85	1	0	1	3	9		

Color : whi. : white, gra. : gray, yel. : yellow, pur. : purple Grain size : si. : silt size, v.f.sd. : very fine sand size, fi.sd. : fine sand size, me.sd. : medium sand size, co.sd. : coarse sand size
Mineral composition : Gl:glass Fl:feldspar Qz:quartz Hm:heavy minerals Ot:others Shape of glass : H:H-type C:C-type T:T-type O:other type
Heavy mineral composition : Bi:biotite Am:amphibole Op:orthopyroxene Cp:clinopyroxene Zi:zircon Ap:apatite Oq:opaque minerals * : less 1% + : common

the gray to white, fine grained lower part 1 cm thick, the white to gray, fine grained upper part 5 cm thick. In the mineral composition, plagioclase and glass are abundant and heavy minerals and quartz are common. Glass particles consist mainly of colorless T-type shards with refractive index of 1.498-1.507. In the heavy minerals, amphibole is dominant, orthopyroxene, biotite and opaque minerals are common and apatite is rare.

K3-351 volcanic ash horizon: The K3-351 volcanic ash horizon, in a silt bed, is composed of 13 per cent volcanic glasses and 3 per cent heavy minerals. In the mineral composition, plagioclase and glass are abundant, heavy minerals are common and quartz is rare. Glass particles consist mainly of colorless T-type and C-type shards with refractive index of 1.498-1.511. In the heavy minerals, biotite, amphibole, apatite, and opaque minerals are dominant and orthopyroxene is common.

K3-334 approximate volcanic ash horizon: The K3-334 approximate volcanic ash horizon, in a marine silt bed, is composed of 10 per cent volcanic glasses and 4 per cent heavy minerals. In the mineral composition, plagioclase and glass are abundant and heavy minerals and quartz are common. Glass particles consist mainly of colorless and pale brown C-type shards with refractive index of 1.499-1.504. In the heavy minerals, amphibole and biotite are dominant, opaque min-

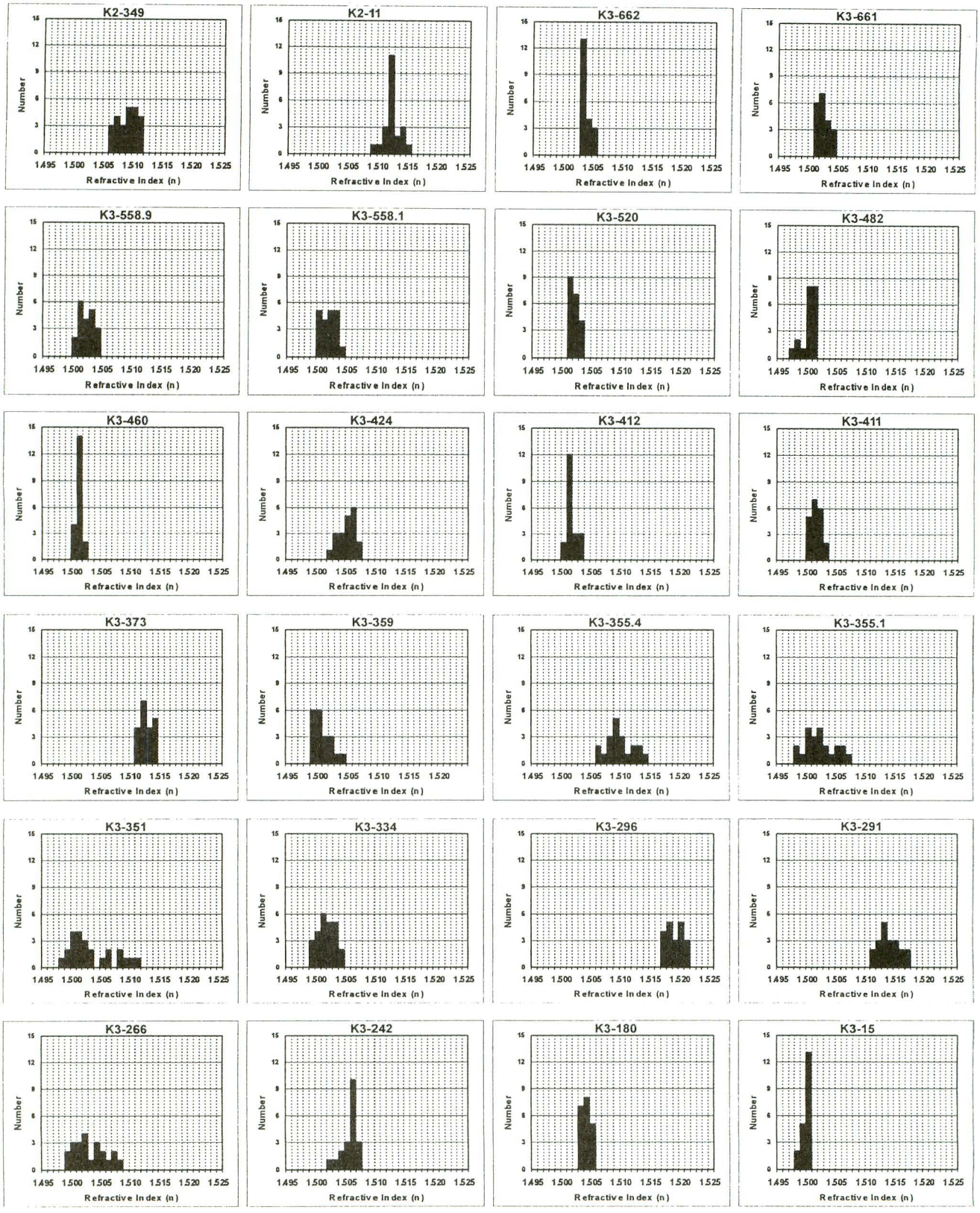

Fig. 6 Distributions of refractive index of volcanic glass.

erals and orthopyroxene are common and apatite is rare.

K3-296 volcanic ash layer: The K3-296 volcanic ash layer, the thickness of which is 8 cm, is composed of gray and fine grained volcanic ash. In the mineral composition, plagioclase and glass are abundant and heavy minerals and quartz are rare. Glass particles con-

sist mainly of colorless and pale brown T-type shards with refractive index of 1.517-1.521. In the heavy minerals, amphibole, orthopyroxene, clinopyroxene and biotite are common.

K3-291 volcanic ash horizon: The K3-291 volcanic ash horizon, in a marine silt bed, is composed of 8 per cent volcanic glasses and single percent heavy minerals. In the mineral composition, plagioclase and glass are abundant and heavy minerals are rare. Glass particles consist mainly of colorless C-type shards with refractive index of 1.511-1.517. In the heavy minerals, amphibole is dominant, opaque minerals and biotite are common, and orthopyroxene, apatite and zircon are rare.

K3-266 approximate volcanic ash horizon: The K3-266 approximate volcanic ash horizon, in a marine silt bed, is composed of 6 per cent volcanic glasses and 2 per cent heavy minerals. In the mineral composition, plagioclase and glass are abundant, heavy minerals are common, and quartz is rare. Glass particles consist mainly of colorless C-type shards with refractive index of 1.499-1.508. In the heavy minerals, amphibole is dominant, opaque minerals and orthopyroxene are common and clinopyroxene, biotite and zircon are rare.

K3-242 volcanic ash layer: The K3-242 volcanic ash layer, the thickness of which is 5 cm, is composed of gray to white and fine grained volcanic ash. In the mineral composition, plagioclase and glass are abundant and quartz is rare. Glass particles consist mainly of colorless H-type and C-type shards with refractive index of 1.502-1.507 (mode : 1.506). In the heavy minerals, amphibole, orthopyroxene and clinopyroxene are dominant and opaque minerals and biotite are common.

K3-195 volcanic ash layer: The K3-195 volcanic ash layer, the thickness of which is 5 cm, is composed of gray and medium to coarse grained volcanic ash. In the mineral composition, plagioclase and heavy minerals are abundant and quartz is rare. In the heavy minerals, amphibole is dominant, orthopyroxene (γ =1.705-1.713) and opaque minerals are common, and apatite is rare. Amphibole particles consist mainly of green and green brown shards with refractive index of 1.681-1.691 (n_2) (mode : 1.683).

K3-180 volcanic ash horizon: The K3-180 volcanic ash horizon, in a silt bed, is composed of 5 per cent volcanic glasses and a single percent heavy min-

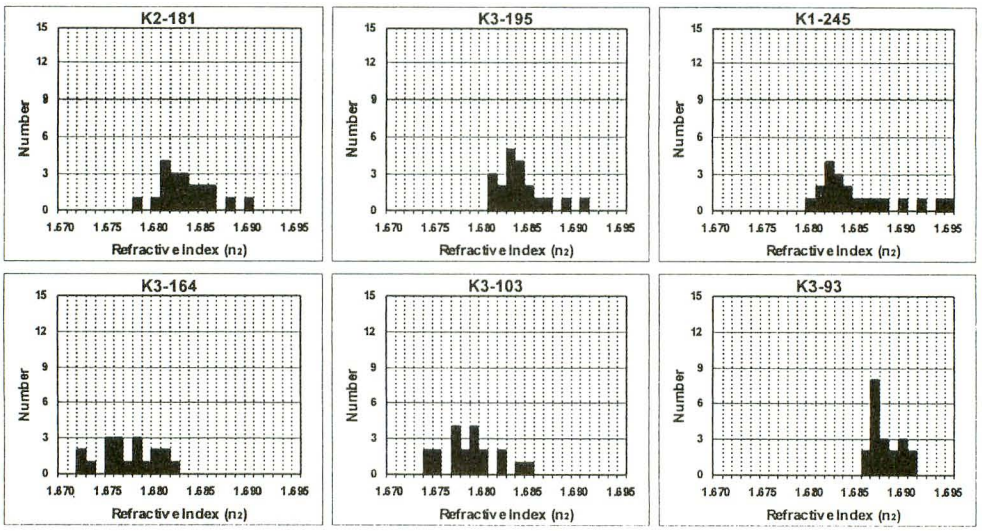

Fig. 7 Distributions of refractive index of amphibole.

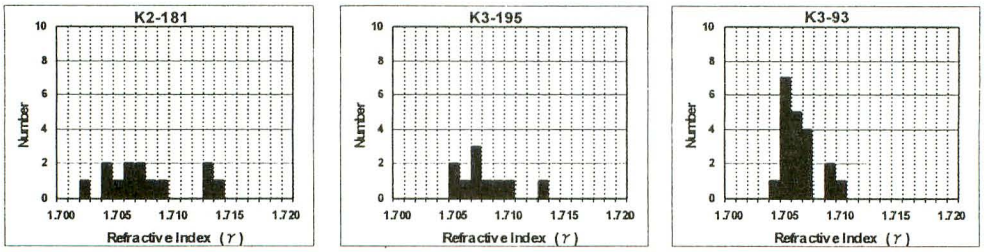

Fig. 8 Distributions of refractive index of orthopyroxene.

erals. In the mineral composition, plagioclase and glass are abundant and heavy minerals and quartz are rare. Glass particles consist mainly of colorless H-type and C-type shards with refractive index of 1.503-1.505. In the heavy minerals, amphibole is dominant, opaque minerals and orthopyroxene are common, and clinopyroxene, biotite and apatite are rare.

K3-164 crystal ash horizon: The K3-164 crystal ash horizon, in a marine sand bed, is composed of 6 per cent heavy minerals. In the heavy minerals, amphibole is dominant, opaque minerals are common, and orthopyroxene is rare. Amphibole particles consist mainly of green and green brown shards with refractive index of 1.672-1.682 (n_2).

K3-103 crystal ash horizon: The K3-103 crystal ash horizon, in a sand bed, is composed of 12 per cent heavy minerals. In the heavy minerals, amphibole is dominant, opaque minerals are common, and orthopyroxene and apatite are rare. Amphibole particles consist mainly of green and green brown shards with refractive index of 1.674-1.685 (n_2).

K3-93 volcanic ash layer: The K3-93 volcanic ash layer, the thickness of which is 8 cm, is composed of pale purplish gray and fine grained volcanic ash. In the mineral composition, plagioclase and heavy minerals are abundant, quartz is common, and glass is very rare. Glass particles consist mainly of colorless C-type shards. In the heavy minerals, amphibole, orthopyroxene (γ=1.704-1.710) and opaque minerals are dominant, clinopyroxene and apatite are common, and biotite and zircon are rare. Amphibole particles consist mainly of green and green brown shards with refractive index of 1.686-1.691 (n_2) (mode : 1.687).

K3-15 volcanic ash horizon: The K3-15 volcanic ash horizon, in a silt bed, is composed of 14 per cent volcanic glasses and a single per cent heavy minerals. In the mineral composition, plagioclase and glass are abundant, and heavy minerals are rare. Glass particles consist mainly of colorless and pale brown H-type shards with refractive index of 1.498-1.500 (mode : 1.500). In the heavy minerals, amphibole, opaque minerals and orthopyroxene are dominant and clinopyroxene is rare.

5. Measurement of the paleomagnetism

The paleomagnetism was measured in the GS-K2 core. Because the GS-K2 core is dominated by sand and gravel, limited horizons are suitable for the paleomagnetic analysis. A total of 14 samples of No. 1 to No. 14 were thus collected from clay and silty clay horizons at depths of 350 to 347 m, 297 to 295 m and 288 to 286 m (Fig. 9). They were given cubic shapes of 10 cm^3 each using non-magnetic knives and kept in acrylic boxes.

Natural remanent magnetization (NRM) of all samples were measured with a 2G super conducting rock magnetometer of Kobe University. To isolate a characteristic remanent magnetization (ChRM) direction, all samples were mainly subjected to progressive demagnetization in alternating field (AF) at 2.5 mT steps up to 10 mT, at 5 mT steps up to 30 mT, and at 10 mT steps higher AF fields until the initial NRM intensity reached 5-10% of the initial value.

The initial NRM intensity of these samples mostly ranged from 10^{-4} to 10^{-3} Am^{-1}. Most of the samples showed little change in direction after removal of vis-

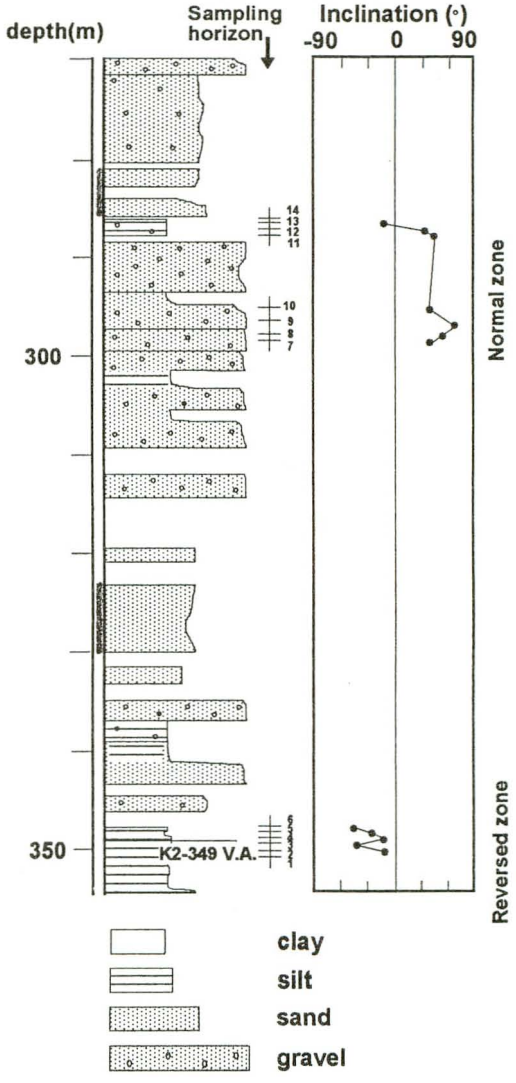

Fig. 9 Palaeomagnetic results in the lower part of the GS-K2 drilling core. The inclination data are of characteristic remanent magnetization.

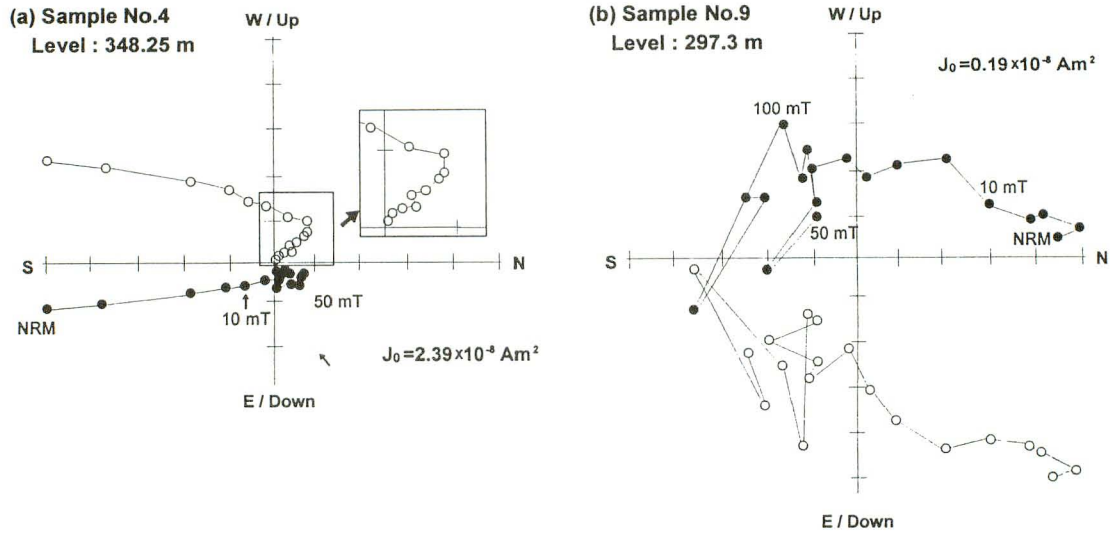

Fig. 10 Representative results of progressive AF demagnetization. ●/○ in the vector end-point diagram represent projection on the horizontal / vertical plane.

cous remanent magnetization at steps of 5-30 mT of AF, as shown by a typical result in Fig. 10 (a). Such a singular component behavior was observed in 3 samples (Sample No. 4, 7, 11), from which a ChRM direction was calculated using principal component analysis (Kirschvink, 1980). On the other hand, 9 samples (Sample No. 2, 3, 5, 6, 8～10, 12, 14) clearly have higher coercivity components that cannot be isolated by the principal component analysis because of their weak remanence intensity. In this study, a remanence direction near the center of the cluster about each of the samples was adopted as a ChRM direction following Biswas et al. (1999), as shown by a typical result in Fig. 10 (b). Other samples (Sample No. 1, 13) showed complicated patterns and were not able to calculate a ChRM directions. Inclination data of ChRMs obtained from 12 samples are plotted in Fig. 9.

6. Discussion

On the basis of the similarities of lithology, petrography and stratigraphic position, the volcanic ash layers and the volcanic ash horizons in the GS-K2 and GS-K3 cores are correlated with each other. These volcanic ashes are also correlated with the known tephra layers of the Osaka Group around the Sennan-Senboku Area (Komyoike Research Group, 1971 ; Yoshikawa, 1973 ; Itihara et al, 1975 ; Yoshikawa, 1984 ; Research Group for the Lowermost Osaka Group, 1992), with those of the Middle to Upper Pleistocene around the Kobe area (Yoshikawa et al, 1993 ; Miyakawa et al, 1996), with those of the subsurface Quaternary sediments of the Osaka Plain (Yoshikawa et al, 1987, 1997, 1998), and especially with those of the GS-K1 core (Yoshikawa et al, 2000) (Table 2). This core was drilled near by the GS-K2 and GS-K3 core sites and provided one of the most detailed tephrostratigraphy of the Osaka sedimentary basin (Fig. 8). On the basis of this tephra correlation and the result of the paleomagnetism of the GS-K2 core, the marine beds in the GS-K2 and GS-K3 cores are assigned to the marine clay beds of the Osaka Group named like the Ma 3.

6-1. Correlation of volcanic ash layers and horizons, and marine beds in the GS-K2 core

The K2-349 volcanic ash horizon is correlated with the K1-422 volcanic ash layer (Yoshikawa et al, 2000), a correlative of the Sayama volcanic ash layer (Yoshikawa, 1973 ; Yoshikawa, 1984). These volcanic ashes include similar types of glass shards (C-type, H-type) with refractive index of 1.506 to 1.511 ; 1.502 to 1.513 ;, and 1.504 to 1.510, respectively.

Kobayashi et al. (2001) correlated the K2-181 volcanic ash layer with the K1-245 volcanic ash layer (Yoshikawa et al, 2000) and with the Kasuri volcanic ash layer (Ishida and Yokoyama, 1969 ; Yoshikawa, 1976). This correlation was confirmed here by the similarities in lithologic properties (white coarse-grained volcanic ashes containing many large heavy minerals), in heavy mineral composition (amphibole>>orthopyroxene), in refractive index of amphibole (1.678 to 1.690 ; 1.680 to 1.695 ; 1.678 to 1.689, respectively) and in refractive index of orthopyroxene (1.702 to 1.714 of the K2-181 and 1.704 to 1.711 of the Kasuri volcanic ash

Table 2 Petrographic properties of volcanic ashes in the GS-K2 and GS-K3 drilling core and their correlatives in the GS-K1 drilling core (Yoshikawa et al., 2000) and the Osaka Groups.

Name of tephra	Glass: Sharp H	C	T	O (%)	Refractive Index (n) (mode)	Heavy mineral composition: Bi	Am	Op	Cp	Zr	Ap	Oq (%)
K2-11	**70**	**28**	**2**	**0**	**1.509-1.515 (1.512)**	**2**	**21**	**40**	**6**	**0**	**1**	**30**
Yoko-oji **(6)**	75	23	2	0	1.509-1.515 (1.511-1.512)	1	17	37	21	1	5	17
K3-15	**63**	**33**	**4**	**0**	**1.498-1.500 (1.500)**	*	**60**	**18**	**1**	**0**	**0**	**21**
K1-26	72	27	1	0	1.499-1.501 (1.500)	0	22	51	11	0	0	16
Heianjingu **(6)**	74	22	3	1	1.498-1.501 (1.500)	1	12	54	17	0	0	15
K3-180	**50**	**48**	**2**	**0**	**1.503-1.505**	**2**	**60**	**10**	**3**	**0**	**1**	**24**
K1-223	35	52	9	3	1.502-1.506 (1.503-1.505)	0	44	41	6	1	1	7
Minatojima I **(5)**	+	+			1.503-1.504 (1.504)	0	60	2	4	*	*	33
K2-181						**0**	**82**	**5**	**0**	**0**	**1**	**12**
K3-195						**0**	**86**	**6**	**0**	**0**	**1**	**7**
K1-245	0	23	77	0	1.511-1.518	0	97	1	0	0	1	1
Kasuri **(1)**						0	92	3	1	0	0	4
K3-242	**51**	**28**	**21**	**0**	**1.502-1.507 (1.506)**	**4**	**48**	**24**	**16**	**0**	**0**	**8**
Sakura **(1)**	54	36	8	0	1.502-1.507	0	51	19	16	1	1	12
K3-291	**13**	**60**	**27**	**0**	**1.511-1.517**	**11**	**67**	**4**	**0**	**2**	**3**	**13**
K1-348	14	59	24	3	1.504-1.518			+				+
Hacchoike II **(1)**	17	57	25	0	1.512-1.518	0	0	54	10	0	0	35
K3-296	**2**	**9**	**89**	**0**	**1.517-1.521**		+	+	+			
K1-351	0	12	78	0	1.519-1.522	2	30	41	8	0	11	8
Hacchoike I **(1)**	0	38	54	7	1.518-1.523	0	28	48	5	0	0	18
K3-355.1	**5**	**16**	**79**	**0**	**1.498-1.507**	**20**	**65**	**5**	**0**	**0**	**3**	**7**
K1-421	2	39	57	2	1.495-1.503 (1.501-1.503)	45	48	1	0	0	5	1
K2-349	**21**	**53**	**26**	**0**	**1.506-1.511**	**27**	**41**	**16**	**1**	**0**	**0**	**15**
K3-355.4	**36**	**34**	**30**	**0**	**1.506-1.514**	*	**12**	**67**	**2**	**0**	**5**	**14**
K1-422	32	38	27	3	1.502-1.513	+	+	+	+		+	+
Sayama (L) **(1)**	28	53	17	3	1.504-1.510 (1.507)	0	5	39	18	0	0	39
K3-359	**4**	**35**	**61**	**0**	**1.499-1.504**	**45**	**38**	*	**0**	*	**0**	**17**
Toyodaike **(4)**	6	11	81	2	1.4975-1.5030 (1.4985)	1	32	0	0	0	*	66
K3-373	**23**	**45**	**29**	**3**	**1.511-1.514**	*	**14**	**50**	**16**	**0**	**10**	**10**
K1-444	37	32	30	1	1.512-1.516	0	11	63	5	0	5	16
Azuki (L) **(1)**	27	55	15	3	1.510-1.516 (1.514)	0	1	49	10	0	1	38
K3-412	**0**	**14**	**86**	**0**	**1.500-1.503 (1.501)**	**8**	**81**	**0**	**0**	**0**	**4**	**7**
K3-411	**0**	**11**	**89**	**0**	**1.500-1.503**	**2**	**87**	**1**	**0**	**0**	**4**	**6**
K1-488	0	3	97	0	1.499-1.502	4	90	0	0	0	1	5
K1-486	0	7	93	0	1.500-1.503 (1.501-1.502)	52	45	0	0	0	2	1
Yamada III **(1)**	1	27	72	0	1.501-1.503	0	92	0	0	0	2	5
K3-424	**47**	**51**	**0**	**2**	**1.502-1.507**	**1**	**66**	**2**	**0**	**0**	**5**	**26**
Yamada I **(1)**	59	35	6	1	1.503-1.506	0	69	16	1	0	0	14
K3-460	**0**	**23**	**77**	**0**	**1.500-1.502 (1.501)**	**1**	**88**	**0**	**0**	**0**	**7**	**4**
K1-537	0	12	88	0	1.501-1.503 (1.502)	4	92	0	0	*	1	3
Komyoike III **(1)**	0	26	74	0	1.500-1.502	2	93	0	0	0	1	4
K3-482	**48**	**43**	**9**	**0**	**1.497-1.501 (1.500-1.501)**	**0**	**83**	**10**	**0**	**1**	**2**	**4**
K1-566	40	40	18	2	1.500-1.502	1	78	11	2	0	4	4
Pink (L) **(1)**	53	35	13	3	1.500-1.501	0	77	11	3	1	3	8
K3-520	**0**	**14**	**85**	**1**	**1.501-1.503**	**1**	**90**	**2**	**0**	**0**	**3**	**4**
K1-610	1	19	80	0	1.500-1.502	1	89	0	0	0	2	8
YU-277 **(3)**						1	96	0	0	0	2	2
OT-161 **(2)**		+	++		1.500-1.503	*	95	0	0	*	1	4
K3-558.9	**3**	**16**	**81**	**0**	**1.500-1.504**	**2**	**87**	**1**	**0**	**1**	**6**	**3**
K3-558.1	**2**	**32**	**64**	**2**	**1.500-1.504**	**1**	**86**	**3**	**0**	**0**	**5**	**5**
K1-648	1	36	67	1	1.501-1.503	6	92	*	0	*	2	*
Yellow II **(1)**					1.497-1.503	0	94	0	0	0	0	6
Yellow III **(1)**	0	20	71	8	1.501-1.503 (1.503)	1	93	0	0	0	0	6
K3-662	**4**	**12**	**84**	**0**	**1.503-1.505 (1.503)**	**1**	**85**	**1**	**0**	**1**	**3**	**9**
K3-661	**0**	**28**	**72**	**0**	**1.501-1.504**	**0**	**86**	**1**	**0**	**1**	**6**	**6**
Senriyama I **(1)**	0	29	69	1	1.503-1.505 (1.504)	0	94	2	0	1	3	3
Senriyama II **(1)**	1	33	65	0	1.500-1.503	0	93	0	0	0	1	5

Shape of glass H:H-type (Ha+Hb) C:C-type (Ca+Cb) T:T-type (Ta+Tb) O:other type (Yoshikawa, 1976)
Heavy mineral composition Bi:biotite Am:amphibole Op:orthopyroxene Cp:clinopyroxene Zi:zircon Ap:apatite Oq:opaque minerals
*:less 1% +:common ++: abundant

(1) Yoshikawa (1984) **(2)** Yoshikawa et al.(1998) **(3)** Yoshikawa et al.(1997) **(4)** Research Group for the Lowermost Osaka Group (1992) **(5)** Miyakawa et al. (1996) **(6)** Yoshikawa et al. (1986)

layer).

The K2-11 volcanic ash horizon is correlated with the Yokooji volcanic ash layer (Yoshikawa et al, 1986). Heavy mineral composition (amphibole, orthopyroxene, clinopyroxene), and dominant types (H-type>C-type) and refractive index (1.509 to 1.515 ; 1.507 to 1.515) of glass shards are similar to each other.

As a result of this tephra correlation, the marine sand bed, at depth of 330.0 to 323.2 m above the K2-349 volcanic ash horizon is correspondent to the Ma 4 bed. The measurement of the paleomagnetism of the GS-K2 core confirms the correlation. Six samples (sample No. 1～6) from 350 to 347 m horizons indicate a trend of reversal-polarity zone, and others (sample No. 7～14) from levels above 300 m show a trend of normal-polarity zone. Because of the Brunhes normal chronozone and Matuyama reversed chronozone (B/M) boundary is fairly well located at the base of the Ma 4 bed (Hayashida and Yokoyama, 1989 ; Biswas et al., 1999), and the marine sand bed at depth of 330.0 to 323.2 m is surely correlative with the Ma 4 bed. It is possible to support this contrast from the similarities of lithology between the GS-K2 core and the GS-K3 core and correspondence of reflectors in the seismic reflection survey section, Ishiyagawa Line (Geo-Database Information Committee of Kansai, 1998).

The K2-181 volcanic ash layer, a correlative with the Kasuri volcanic ash layer, occurs in or immediately below the Ma 8 bed (Ishida and Yokoyama, 1969 ; Yoshikawa, 1976). Therefore, two marine sand beds above the Ma 4 bed at depths of 286.0 to 280.6 m and 246.2 to 239.5 m are assigned to two of the Ma 5, Ma 6 and Ma 7 beds.

6-2. Correlation of volcanic ash layers and horizons, and marine beds in the GS-K3 core

In the K3-L unit (680 to 598.4 m), Geo-Database Information Committee of Kansai (1998) suggested that the K3-662 and K3-661 volcanic ash layers were correlated with the Senriyama I and II volcanic ash layers (Yoshikawa, 1976), respectively, in spite of the detailed analyses of the former two tephra layers. Our results confirm their correlation. The K3-662 and Senriyama I volcanic ash layers are very similar in heavy mineral composition (amphibole dominant), in shape type (T-type>>C-type) and refractive index (n=1.503-1.505) of glass shards. The K3-661 and Senriyama II volcanic ash layers also have similar characteristics like heavy mineral composition (amphibole dominant), glass shard morphology (T-type>>C-type), and refractive index of glass shards (n=1.501-1.504, 1.500-1.503).

In the K3-M unit (598.4 to 227.7 m), Geo-Database Information Committee of Kansai (1998) proposed the following correlation of volcanic ash layers:

- K3-482, K1-566, and the Pink (Itihara et al, 1955) volcanic ash layers,
- K3-460, K1-537, and the Komyoike III (Yoshikawa, 1973) volcanic ash layers,
- K3-424 and the Yamada I (Itihara et al., 1975) volcanic ash layers,
- K3-412 and K3-411 are correlated with K1-488 and K1-486, respectively, and one of this paired ashes is correlative to the Yamada III volcanic ash layer (Itihara et al., 1975),
- K3-373, K1-444, and the Azuki (Itihara et al, 1955) volcanic ash layers,
- K3-296, K1-351, and the Hacchoike I (Itihara et al, 1955) volcanic ash layers.

The volcanic ash layers named like the K1-566 herein are after Yoshikawa et al. (2000). The tephra correlation is supported by the similarities of heavy mineral compositions, glass shard morphology, and refractive index of glass shards among the individual correlative volcanic ash layers (Table 2).

Previous studies revealed the relative stratigraphy of the volcanic ash layers to the marine clay beds of the Osaka Group. The Pink volcanic ash layer occurs above the Ma1 bed (Yoshikawa, 1976). The Yamada I, Azuki, and Hacchoike I volcanic ash layers occur in the Ma2, Ma3, and Ma5 beds, respectively (Yoshikawa, 1976; Itihara et al, 1955). Consequently, the marine beds of the K3-M unit at depths of 500.2 to 489.2 m, 426.8 to 418.0 m, 380.5 to 360.0 m, 339.8 to 323.4 m, and 296.8 to 289.5 m, are equivalents of the Ma1, Ma2, Ma3, Ma4, and Ma5 beds, in ascending order. Between the Ma1 and Ma2 beds, two thinner marine beds are recognized in the K3-M unit at depths of 469.8 to 456.6m and 452.6 to 450.4m. Compared with the detailed stratigraphy of the marine clay beds of the Osaka Group (Yoshikawa et al., 1997, 1998), the two marine beds are correlative to the Ma1.3 and Ma1.5 beds, respectively.

In addition to the correlation, four volcanic ash layers and three volcanic ash horizons of the K3-M unit are newly correlated with known tephra layers (Table 2). In the K3-U unit, one volcanic ash layer and two volcanic ash horizons are also identified with well-known tephra layers (Table 2).

1) Either of K3-558.9 and K3-558.1, K1-648, and either of the Yellow II and III (Komyoike Research Group, 1971) volcanic ash layers

These five volcanic ash layers have similar petro-

graphic characteristics. They are all mainly composed of heavy minerals dominated by amphibole and glass shards (T-type>C-type) with almost same ranges of refractive index (Table 2). Further information like major and trace element compositions of glass shards is needed for detailed correlation of each of the five volcanic ash layers. The Yellow II and III volcanic ash layers occur in the middle part of the Ma0 bed (Komyoike Research Group, 1971), and thus the marine beds at depths of 598.4 to 590.2 m and 559.2 to 550.2 m are assigned to the Ma-1 and Ma0 beds, respectively.

2) K3-520, K1-610, YU277 (Yoshikawa et al., 1997) and OT161 (Yoshikawa et al., 1998) volcanic ash layers

These volcanic ash layers are correlated with each other, because they are similar in heavy mineral composition (amphibole dominant), glass shard type (T-type>>C-type), and refractive index of glass shards (n=1.501-1.503 in K3-520, 1.500-1.502 in K1-610, and 1.500-1.503 in OT161). A stratigraphic position of every ash layer intercalated below the Pink volcanic ash layers is also consistent with this correlation. Because the OT161 occurs in the lower part of the Ma0.5 bed (Yoshikawa et al, 1998), the marine bed of 520.0 to 517.0 m corresponds to the Ma0.5 bed.

3) K3-359 volcanic ash horizon and the Toyodaike volcanic ash layer (Research Group for the Lowermost Osaka Group, 1992)

Heavy mineral composition is characterized by a combination of amphibole, opaque minerals and biotite in the two volcanic ashes. They have similar glass shard morphology (T-type>C-type) and refractive index of glass shards (n=1.499-1.504, 1.497-1.503). Further, these volcanic ash horizons are above the Azuki volcanic ash layer (Research Group for the Lowermost Osaka Group, 1992). Accordingly, the K3-359 volcanic ash horizon and the Toyodaike volcanic ash layer are correlated with each other.

4) K3-355.4 volcanic ash horizon, K1-422 volcanic ash layer, and the Sayama volcanic ash layer (Yoshikawa, 1973)

These volcanic ashes are similar in heavy mineral composition (orthopyroxene>amphibole), glass shard type (C-type>H-type,T-type), and refractive index of glass shards (n=1.506-1.514, 1.502-1.513, 1.504-1.510). The stratigraphic levels of the two volcanic ashes permit this correlation, as they occur above the Azuki and Toyodaike volcanic ash layers (Research Group for the Lowermost Osaka Group, 1992).

5) K3-355.1 and K1-421 volcanic ash layers

The K3-355.1 and K1-421 are correlative volcanic ash layers, because of similar heavy mineral compositions (amphibole>biotite), glass shard morphology (T-type>C-type), and refractive index of glass shards (n=1.498-1507, 1.495-1.503), as well as of the same stratigraphic level above the Sayama volcanic ash layer.

6) K3-291 volcanic ash horizon, K1-348 volcanic ash layer, and the Hacchoike II volcanic ash layer (Itihara et al., 1975)

All the volcanic ashes occur just above the Hacchoike II volcanic ash layer. They are similar in shape (C-type>>T-type>H-type) and refractive index (n=1.511-1.517, 1.504-1.518, 1.512-1.518) of glass shards. Heavy mineral composition of the K3-291 is different from that of the K1-348 or the Hacchoike II volcanic ash layer; the former is dominated by amphibole and biotite crystals (Table 2). Heavy minerals are very rare in the K3-291 (only 1%) and thus the different composition is probably due to contamination.

7) K3-242 and the Sakura (Itihara et al., 1975) volcanic ash layers

These volcanic ash layers are correlated with each other, because of the good similarities of heavy mineral compositions (amphibole>orthopyroxine>clinopyroxine), glass shard types (H-type>C-type>T-type), and refractive index of glass shards (n=1.502-1.507). From the stratigraphic position of the Sakura volcanic ash layer immediately below the Ma7 bed (Yoshikawa, 1984), the marine beds of 268.9 to 259.5m and 242.8 to 236.4 m are equivalent to the Ma6 and Ma7 beds, respectively.

8) K3-195, K1-245, and the Kasuri (Ishida and Yokoyama, 1969) volcanic ash layers

Kobayashi et al. (2001) indicates that these volcanic ash layers were correlated with each other. They have unique lithologic properties (white coarse-grained volcanic ash containing many large amphibole crystals), and are similar in heavy mineral composition (amphibole>>orthopyroxene). Refractive index of amphibole and orthopyroxene are n_2 = 1.681-1.691 and γ =1.705-1.713 in the K3-195, n_2 = 1.680-1.695 and γ =1.704-1.711 in the K1-245, and n_2 =1.678-1.689 and γ =1.705-1.710 in the Kasuri volcanic ash layer (Yoshikawa, 1976). This result confirms the correlation of the three volcanic ash layers.

9) K3-180 volcanic ash horizon, K1-223 volcanic ash layer, and the Minatojima I volcanic ash layer (Miyakawa et al., 1996)

The K3-180 and the Minatojima I volcanic ash layers have very similar heavy mineral compositions (amphibole>opaque minerals>orthopyroxene), but the K1-223 has slightly different heavy mineral composi-

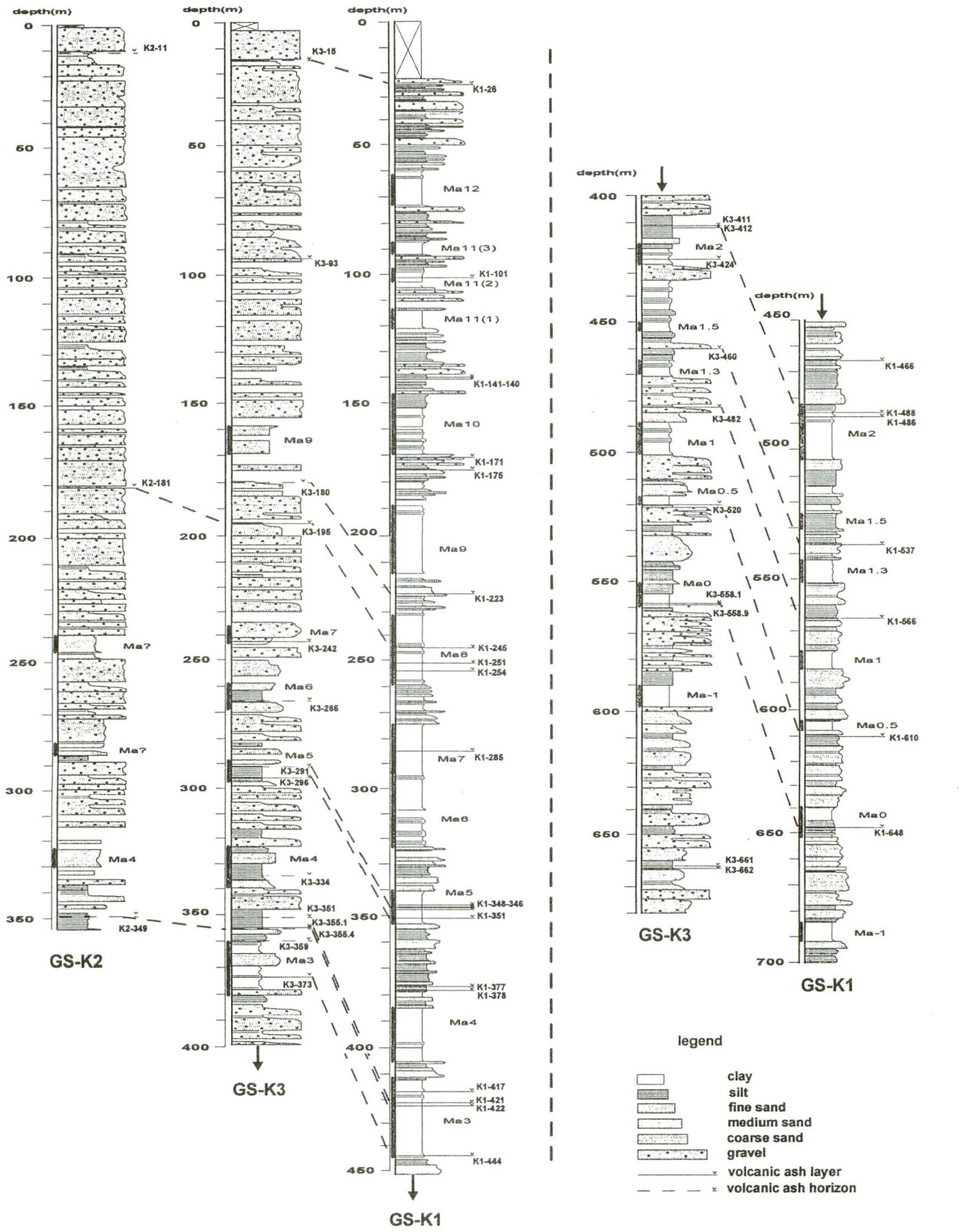

Fig. 11 Geologic correlation among the GS-K2, GS-K3 and GS-K1 drilling cores.

tion. All the volcanic ashes, however, are similar in glass shard shape (H-type and C-type) and refractive index of glass shards (n=1.503-1.505, 1.502-1.506, 1.503-1.504). Accordingly, the former two volcanic ashes are identified with the Minatojima I volcanic ash layers. The Minatojima I volcanic ash layer occurs below the Ma9 bed or in the lowermost part of the Ma9. Thus, the marine sand bed of the K3-U unit at depths of 168.9 to 158.9 is correspondent to the Ma9 bed.

10) K3-15 volcanic ash horizon, K1-26 volcanic ash layer, and the Heian-jingu volcanic ash layer (Yoshikawa et al., 1986)

These volcanic ashes are correlated with each other because they are similar in heavy mineral composition (orthopyroxene>opaque minerals, amphibole, clinopyroxene) and glass shape type (H-type>>C-type). Refractive index of glass shards also show similar values (n=1.498-1.500, 1.499-1.501).

The K3-164 and K3-103 horizons indicate peaks of heavy mineral contents (Fig. 5). Heavy mineral particles in these horizons are mainly composed of fresh amphibole crystals with enhedral shapes. The Rokko Mountains are mainly underlain by the Tamba and Arima Groups and Granitic rocks that sparsely contain amphibole crystals (Huzita and Kasama, 1983). After all, the fresh amphibole crystals appear to be derived not from such basement rocks but from volcanic ash layers and the two horizons enriched with the fresh heavy minerals possibly indicate volcanic ash horizons rich in heavy mineral crystals.

Correlation of volcanic ash layers and horizons and marine beds of the GS-K2 and GS-K3 cores with those of major deep drilling cores in the Kobe area and the Osaka Plain including the GS-K1 core is summarized in Fig. 11.

7. Conclusion

Quaternary stratigraphy in the GS-K2 core and in the upper part of the GS-K3 core are examined by describing the properties of volcanic ash layers and volcanic ash horizons and measuring the paleomagnetism. As the result, in the GS-K2 core, 2 volcanic ash horizons were identified at depths of 349 m and 11 m, as well as a volcanic ash layer at depth of 181 m. The K2-349 volcanic ash horizon is correlated with the Sayama volcanic ash layer for the similarities of shapes of glass shards and its refractive index. As a result of this correlation, the marine sand bed, at depth from 330.0 to 323.2 m, corresponds to the Ma 4 bed. The measurement of the paleomagnetism of the GS-K2 core confirms the marine sand bed correlation with the Ma 4 bed. In the GS-K3 core, 16 volcanic ash layers were found and 6 volcanic ash horizons, 2 approximate volcanic ash horizons and 2 crystal ash horizons were determined. Four volcanic ash layers and 3 volcanic ash horizons in the K3-M unit and one volcanic ash layer and 2 volcanic ash horizons in the K3-U unit are newly correlated with known volcanic ash layers. The volcanic ashes of the K3-558.9/K3-558.1, K3-520, K3-359, K3-355.4, K3-355.1, K3-291, K3-242, K3-195, K3-180 and K3-15 are equivalent with the K1-648/Yellow II/III, K1-610/YU277/OT161, Toyodaike, K1-422/Sayama, K1-421, K1-348/Hacchoike II, Sakura, K1-245/Kasuri, K1-223/Minatojima I and K1-26/Heian-jingu volcanic ash layers, respectively. On the basis of these tephra correlations, 12 marine beds of the K3-M and K3-U are equivalents of the Ma -1, Ma 0, Ma 0.5, Ma 1, Ma 1.3, Ma 1.5, Ma 2, Ma 3, Ma 4, Ma 5, Ma 6, Ma 7, and Ma 9, in ascending stratigraphic order. These correlations of the marine beds are very important indicators of core sediments and available for considering the vertical change of lithofacies.

Acknowledgments

We express our deep thanks to Professor Hisao Kumai of Osaka City University and senior inspector Kiyohide Mizuno of the Geological Survey of Japan for reviewing and improving the manuscript. We also thank graduate students of Kobe University, especially for Takashi Kirimoto for assisting in sampling for the measurement of paleomagnetism.

References

Biswas, D.K., Hyodo, M., Taniguti, Y., Kaneko, M., Katoh, S., Sato, H., Kinugasa, Y. and Mizuno, K. (1999) Magnetostratigraphy of Plio-Pleistocene sediments in a 1700-m core from Osaka Bay, southwestern Japan and short geomagnetic events in the middle Matuyama and early Brunhes chrons. Palaeogeography, *Palaeoclimatology, Palaeoecology*, **148**, 233-248.

Furutani, M. (1989) Stratigraphical subdivision and pollen zonation of the Middle and upper Pleistocene in the coastal area of Osaka Bay, Japan. *J. Geosci., Osaka City Univ.*, **32**, 53-83.

Geo-Database Information Committee of Kansai (1998) *Ground of Kansai area especially Kobe and Hanshin, Osaka*, Yodogawa kogisya, 270p.**

Hayashida, A. and Yokoyama, T. (1989) Brunhes/

Matuyama polarity epoch boundary in the Osaka Group of the Senriyama Hills, southwest Japan. *Palaeogeogr., Palaeoclimatol., Palaeocol*, **72**, 195-201.

Huzita, K. and Kasama, T. (1983) Geology of the Kobe District, Quadrangle Series, Scale 1:50000. Geological Survey of Japan, Tsukuba, 115p.**

Ikebe, N., Iwatsu, J. and Takenaka, J. (1970) Quaternary geology of Osaka with special reference to land subsidence. *J. Geosci., Osaka City Univ.*, **13**, 39-98.

Ishida, S. and Yokoyama, T. (1969) Tephrochronorogy, paleogeography and tectonic development of Plio-Pleistocene in Kinki and Tokai Districts, Japan. *The Quat. Res. (Daiyonki-Kenkyu)*, **9**, 3-4, p.101-112.*

Ishihara, N., Mitamura, M., Tanaka, Y. and Kinugasa, Y. (1997) Volcanic glass analysis on the shallow part of the drilling core at the GS-K4 site, Nagata-ku, Kobe City, Japan. *The Proceedings of the 7th Symposium on Geo-environments and Geo-technics*, 1997, p.331-336.*

Itihara, M. (1960) Some problems of the Quaternary sedimentaries in the Osaka and Akashi Areas. *Earth Sci. (Chikyu-Kagaku)*, **49**, 15-25.*

Itihara, M. (Ed.), (1993) The Osaka Group. Sogensha, 340p.*

Itihara, M., Huzita, K., Morishita, A. and Nakaseko, K. (1955) Stratigraphy of the Osaka Group in the Senriyama Hills - Study on the Osaka Group (Part 1)-. *J. Geol. Soc. Japan*, **61**, 433-441.*

Itihara, M., Yoshikawa, S., Inoue, K., Hayashi, T., Tateishi, M. and Nakajima, K. (1975) Stratigraphy of the Plio-Pleistocene Osaka Group in Sennan-Senpoku Area, South of Osaka, Japan. *J. Geosci., Osaka City Univ.*, **19**, 1-29.

Itihara, M., Yoshikawa, S., Kamei, T. and Nasu, T. (1988) Stratigraphic subdivision of Quaternary deposits in Kinki district, Japan. *Mem. Geol. Soc. Japan (Chishitsugaku Ronshu)*, **30**, 111-125.*

Kajiyama, H. and Itihara, M. (1972) The Developmental History of the Osaka Plain with References to the Radio-carbon Dates. *The Memoirs of the Geological Society of Japan*, **7**, 101-112.*

Kirschvink, J.L. (1980) The least-squares line and plane and the analysis of paleomagnetic data. *Geophys. J. R. Astron. Soc.* **62**, 699-718.

Kobayashi, G., Mitamura, M. and Yoshikawa, S. (2001) Lithofacies and sedimentation rate of Quaternary sediments from deep drilling cores in the Kobe area, Southwest Japan. *Earth Sci. (Chikyu-Kagaku)*, **55**, 131-143*

Komyoike Research Group (1971) The Osaka Group around Komyoike in the Shinodayama Hills, south of Osaka. *Earth Sci. (Chikyu-Kagaku)*, **25**, 201-210.*

Mitamura, M., Takemura, K., Kitada, N. and Saito, R. (2000) Subsurface Geology Reviewed with Drilling Data in the Kobe - Hanshin Region, Central Japan. *The Quat. Res. (Daiyonki-Kenkyu)*, **39**, 319-330.*

Mitamura, M., Yoshikawa, S., Ishii, Y., Kaito, S. and Nagahashi, Y. (1998) Lithology on the OD Drilling cores in the Osaka Plain. *Bull. Osaka Museum of Natural History*, **52**, 1-20.*

Miyakawa, C., Yoshikawa, S. and Ikeda, Z. (1996) Tephrostratigraphy of Middle to Upper Pleistocene core-sample from the Port Island, Kobe City, Kinki District, Japan. *Earth Sci. (Chikyu-Kagaku)*, **50**, 456-465.*

Research Group for the Lowermost Osaka Group (1992) "Shiba and Manchidani unconformities" in the Osaka Group -The Osaka Group in the northern part of Matsuo Hills, south of Osaka-. *Earth Sci. (Chikyu-Kagaku)*, **46**, 209-220.*

Takemura, K., Katoh, S., Inoue, Y., Ishizawa, K., Ohshika, A., Herai, M., Nojiri, S., Danhara, T., Hayashida, A. and Sano, M. (1997) Stratigraphy of subsurface sediments in the south of Rokko Mountains: drilling samples from Maya Wharf and Higashinada, Kobe City, Japan. In: Museum of Nature and Human Activities, Hyogo: The Great Hanshin-Awaji Earthquake Disaster and Rokko Movements. Rokko Civil Engineering Office, Kobe, 10-56.**

Yoshikawa, S. (1973) The Osaka Group in the south-east of Osaka. *J. Geol. Soc. Japan*, **79**, 33-45.*

Yoshikawa, S. (1976) The volcanic ash layer of the Osaka Group. *J. Geol. Soc. Japan*, **82**, 479-515.*

Yoshikawa, S. (1981) Volcanic glass in the Pleistocene to Holocene sediments in the Osaka Plain. *The Quat. Res. (Daiyonki-Kenkyu)*, 20, 75-87.*

Yoshikawa, S. (1984) Volcanic ash layers in the Osaka and Kobiwako Groups, Kinki District, Japan. *J. Geosci., Osaka City Univ.*, **27**, 1-40.

Yoshikawa, S. and Mitamura, M. (1999) Quaternary stratigraphy of the Osaka Plain, central Japan and its correlation with oxygen isotope record from deep sea cores. *J. Geol. Soc. Japan.*, **105**, 332-340.*

Yoshikawa, S., Mitamura, M., Nakagawa, K., Nagahashi, Y., Iwasaki, Y., Echigo, T., Tsujie, K. and Kitada, N. (1998) Lithostratigraphy and tephrostratigraphy of the Tsumori, Otemae and Hama drilling cores in the Osaka Plain, central

Japan. *J. Geol. Soc. Japan*, **104**, 462-476.*

Yoshikawa, S., Mizuno, K., Katoh, S., Satoguchi, Y., Miyakawa, C., Kinugasa, Y., Mitamura, M. and Nakagawa, K. (2000) Stratigraphy and correlation of the Pleistcene volcanic ash layers from a 1,700m core taken from Higashinada, Kobe City, Southwest Japan. *The Quat. Res. (Daiyonki-Kenkyu)*, **39**, 505-520.*

Yoshikawa, S., Nakagawa, K., Kawabe, T., Furutani, M. and Daishi, M. (1987) Reinvestigation of the deep drilling cores OD-2 and OD-1 in Osaka City, central Japan. *J. Geol. Soc. Japan.*, **93**, 653-655.*

Yoshikawa, S., Nasu, T., Taruno, H. and Furutani, M. (1986) Late Pleistocene to Holocene volcanic ash layers in central Kinki district, Japan. *Earth Sci. (Chikyu-Kagaku)*, **40**, 18-38.*

Yoshikawa, S., Ogura, H. and Fukunishi, S. (1993) The Middle and Upper Pleistcene tephrostratigraphy under the Osaka Plain, central Japan. *J. Geol. Soc. Japan.*, **99**, 467-478.*

Yoshikawa, S., Tsukuda, E., Mitamura, M., Nakagawa, K., Mizuno, K., Higashiwaki, A., Kataoka, K. and Takahashi, M. (1997) litho- and tephrostratigraphy of the Yuhigaoka boring cores from the Osaka Plain, central Japan. *Bull. Geol. Surv. Japan*, **48**, 661-672.*

* in Japanese with English abstract

** in Japanese

Manuscript received August 31, 2001.
Revised manuscript accepted November 12, 2001.